International Journal of Multidisciplinary Research in Biotechnology, Pharmacy, Dental and Medical Sciences (IJMRBPDMS)

Craniofacial Anthropometry and Single Nucleotide Polymophysm as Differential Identification Tools for Idomas and Igedes Population of Benue State

Boniface Adakole Onoja[1], Kareem Suwebat Bidemi[1], Alabi Ade Stephen[1], Imam Aminu[1], Samuel A. Agada[3], Daniel E. Uti[3], Ajao Moyosore Salihu[1]

[1]Department of Anatomy, Faculty of Basic Medical Sciences, University of Ilorin, Kwara State, Nigeria.
22-68le001pg@students.unilorin.edu.ng, kareem.sb@unilorin.edu.ng, alabi.as@unilorin.edu.ng, imam.a@unilorin.edu.ng, moyosoreajao@unilorin.edu.ng.
[2]Department of Human Anatomy, Federal University of Health Sciences Otukpo, Benue State, Nigeria
Veritas University Abuja, Nigeria:
[3]Department of Biochemistry, Faculty of Basic Medical Sciences, College of Medicine, Federal University of Health Sciences, Otukpo, Benue State, Nigeria:
agadasamuel22@gmail.com, (dan4uti@gmail.com, daniel.uti@fuhso.edu.ng)

ABSTRACT

Background: Craniofacial characteristics vary significantly across human populations due to genetic and environmental influences. Although such variations have been widely studied globally, there is limited data on African populations. This study aimed to investigate craniofacial genetics as a tool for differential identification among the Idoma and Igede ethnic groups in Nigeria. Specifically, the study sought to: (i) calculate craniofacial indices from facial image measurements; (ii) identify single nucleotide polymorphisms (SNPs) in the PAX3 and BMP4 genes associated with facial morphology; and (iii) evaluate the relationship between these genetic variations and observable craniofacial traits.

Methods: This study was conducted in two phases. The first phase involved an anthropometric survey of 3,000 randomly selected participants aged 15–30 years. Sample size was determined using Fisher's formula for large populations ($N = Z^2Pq/d^2$). Demographic data were collected using semi-structured questionnaires. Standardized facial photographs were analyzed using Digimizer software to obtain measurements including facial height, bizygomatic width, nasal dimensions, intercanthal distance, and ear size. Data were analyzed using IBM SPSS version 23.0 at a 95% confidence interval.

The second phase involved molecular analysis. DNA samples were collected via buccal swabs. Target regions of the PAX3 and BMP4 genes were amplified using polymerase chain reaction (PCR), followed by purification and sequencing. Sequences were compared with reference data from the NCBI human genome database.

Results: Facial indices were 88.45 ± 4.72 (Idoma males) and 87.81 ± 4.55 (Igede males), and 85.67 ± 4.28 (Idoma females) and 86.12 ± 4.41 (Igede females). Nasal indices ranged from 92.34 ± 6.85 to 95.67 ± 6.78 across both groups. Canthal indices ranged from 37.45 ± 2.65 to 38.56 ± 2.72, while ear indices ranged from 55.98 ± 3.69 to 57.23 ± 3.94. Very long facial types predominated in both populations. Broad and flat nasal types were most common, while intermediate eye types (canthal index 37–46) and large ear sizes were predominant across sexes. Genetic analysis identified 34 nucleotide substitution mutations in the PAX3 gene and 22 in the BMP4 gene. Individuals carrying these mutations exhibited distinct craniofacial measurement patterns compared to the general population.

Conclusion: The integration of craniofacial morphometric analysis with genetic profiling provides a valuable and reliable approach for forensic identification among Idoma and Igede populations. Incorporating genetic markers such as PAX3 and BMP4 into forensic protocols may enhance the identification of both living individuals and human remains.

Keywords: *Craniofacial indices; PAX3; BMP4; single nucleotide polymorphisms; forensic identification; anthropometry; Idoma; Igede; genetic variation; Nigeria.*

Article Info
Received: 05 June 2026, received in revised form: 15 July 2026, accepted: 20 July2026, available online: 27 July 2026; Volume: 2; Issue: 7; Pages: 01-28.

Citation: Onoja B, A., 2026. Craniofacial Anthropometry and Single Nucleotide Polymophysm as Differential Identification Tools for Idomas and Igedes Population of Benue State. *International Journal of Multidisciplinary Research in Biotechnology, Pharmacy, Dental and Medical Sciences (IJMRBPDMS)* 2(7): 01-28.
DOI:

Introduction

Craniofacial genetics is the science of forensic application of deferential identification using the facial measurement and single nucleotide polymorphism as a tool for differential identification especially in the fields of anthropology which has been well documented (Barash *et al*., 2018).

Facial measurements and Single Nucleotide Polymorphism (SNP) analysis have proven to be highly effective in differential identification, particularly in forensic science and anthropology. These methodologies are instrumental in ancestry and genetic research, offering a powerful combination of morphological accuracy and genetic detail. When combined, they allow researchers to generate comprehensive physical and genetic profiles, significantly improving the precision of individual identification (Pollard *et al*., 2022; Richmond *et al*., 2018).

Facial anthropometry provides a precise framework for facial dynamics (Pollard *et al*., 2022; Richmond *et al*., 2018). The human face, often considered a genetic archive, reflects key details related to sex, health, ancestry, kinship, and environmental influences (Claes *et al*., 2014).

Alongside traditional anthropometric methods, advances in molecular genetics, such as SNP and GWAS analysis, present new opportunities to explore ancestral lineages within populations (Golmei *et al*., 2024). These methods have proven potentials to uncover the complex relationship between facial measurements and DNA patterns across the world and this can be explored in sub-saharan africa especially in Nigeria, Sub-Saharan Africa,

As violent crimes, road traffic accidents, war-related disasters, and other crises like fires, floods, border disputes, human trafficking, and terrorism increase, the need for identifying individual remains has grown (Alvarez-Cubero *et al*., 2018).

The identification of severely decayed, mutilated, or skeletal remains is critical for both humanitarian and legal reasons, especially in multi-casualty events and the rising occurrences of missing persons and unclaimed bodies often result in unregistered mass burials. (de Boer *et al*., 2019). Effective identification tools are essential for fostering peace and providing closure for families and societies affected by these tragedies.

Prior studies have established associations between genetic variations and common differences in facial morphology in other part of the world (Barash *et al*., 2016; Qian *et al*., 2022).

The rise in violence, criminal activities, and large-scale disasters, including those caused by war, fires, floods, land disputes, human trafficking, terrorism, and kidnappings, often leads to undocumented deaths and insufficient evidence for identifying individuals. This lack of identification hampers justice and disrupts peaceful conflict resolution. Moreover, little attention has been given to evaluating the reliability and accuracy of 2-dimensional morphologic facial analysis and genetic markers in identifying the typical craniofacial morphology of sub-saharan African particularly among Nigerian population (Esomchi *et al*., 2026). Therefore, research focused on determining the normal craniofacial structure and the genetic markers associated with it with the use of 3-dimensional morphologic facial analysis would significantly improve identification efforts.

Materials and Methods

Ethical Consideration and Consent

The University of Ilorin Ethical Committee, through the Faculty of Basic Medical Sciences Ethical Review Committee, gave their Ethical approval. The reference number for this approval is UERC/ASN/2025/3143. Each participant also gave their informed consent after being told what the research is about and how it will help the community and society as a whole. This study employed both qualitative and quantitative research methodologies via the distribution of a semi-structured questionnaire. While conducting this study, the following ethical principles were taken into account: beneficence, non-maleficence, autonomy, and justice.

Beneficence: The study made sure that the participants' interests were taken into account by making sure that the results would be good for both the people being studied and the country as a whole. To preserve and defend the rights of the participants, moral principles were also taken into account (Anabo *et al*., 2019).

Non-maleficence: the study made sure that the participants didn't get hurt by not causing them pain or suffering during the research process ((Anabo *et al*., 2019).

Autonomy: The study afforded participants the opportunity to make an educated decision regarding their participation, as well as the option to withdraw at any point if they were unable to proceed(Anabo *et al*., 2019).

Justice study was fair since all of the subjects were treated the same way. No one was treated differently than anyone else (Anabo *et al*., 2019).

Research Materials and Equipment

Compared to other advanced imaging methods like computed tomography (CT) scan and magnetic resonance imaging (MRI), 2D photo-image analysis allows for faster image processing and the use of less expensive equipment (Mehta *et al*., 1997). Consequently, photography was factored into this research. The Digimizer software program (version 5.3.5, MedCalc, Belgium) made it easy to measure and calculate all the indices used in this study, even though measuring the 14 craniofacial distances for each participant took a lot of time and effort. However, the outcomes from these instruments are reproducible and can be

preserved for an extended duration, in contrast to direct measurements (e.g., the use of vernier calipers, rulers, etc.), where the investigator lacks access to the volunteers post-initial measurement (Mehta *et al*., 1997).

The study used the following tools and materials:

1. **For the measurements of the head and face:** The Amkov 3.0 Super Amoled 24 Mega Pixel Digital Camera (x4 Zoom), Digimizer software (version 5.3.5, MedCalc, Belgium), a tripod stand (DSLR Camera holder), a stadiometre rule (2 metre Stature Meter), and a weighing scale (Toughened Glass Electronic Digital Scale-LWG-2018A) were used.
2. **For the genetic analysis research:** A genomic DNA extraction kit from NORGEN Biotek Corp., genomic DNA purification kits from Qiagen, buccal swab sticks, micropipettes of different sizes, micropipette tips of different sizes, different buffer solutions, sterile gloves, and different machines were used.

Study Design

Participants for the study were recruited using stratified random sampling techniques.

Study Population

The research was conducted with students from the Idomas and Igedes ethnic groups at the Federal University of Health Sciences Otukpo and college of Education Oju in Nigeria. The participants in the study comprised both males and females aged 15 to 29 years. To gather biodata, 3000 healthy volunteers without apparent facial abnormalities were selected through semi-structured, self-administered questionnaires. The WHO classification put the participants into three age groups.

Group 1: Adolescent 15 to 19

Group 2 is made up of people who are 20 to 24 years old (young adults).

Group 3: Adults ages 25 to 29

Research Population and Sample Size Determination

According to the Academic Record office at the Federal University of Health Sciences Otukpo and college of Education Oju the population of freshly registered students were about 7000 and 5000 respectively for the 2024–2025 academic session, which was when recruitment took place.

Sample Size (SS) Determination

The sample size was determined using the fischer's formular for population greater than (10,000) as follow:

$$SS = \frac{(Z^2 \times pq)}{d^2}$$

Were SS desired sample sizesss

Z = 1.96 (at 95% C.1),

- p= proportion of the target population to have characteristics being measured from previous study. (Idoma and Igede population constitutes 1.6% and 0.2% of Nigeria population respectively). Map of Nigeria showing major ethnic groups (percentage of population) (Johnie, 2011). Following the method adopted by (David *et al*., 2020).
- Therefore, p=0.5
- d= error margin (error limit 0.05)

Therefore, SS= $(1.96^2 \times 0.5 \times 0.5) / (0.063^2)$

$$SS = \frac{3.8416 \times 0.5 \times 0.5}{(0.063) \times (0.063)}$$

$$SS = \frac{0.9604}{0.003969}$$

$$SS = 242.975309$$

Sampling Technique and Subject Selection.

Sampling Technique

Volunteers who fulfilled the inclusion criteria were randomly chosen by a stratified random sample method from the Idomas and Igedes ethnic groups of Nigeria.

Inclusion Criteria

The volunteers, aged 18 to 30, belonged to the pure Idomas and Igedes ethnic groups, traceable to their grandparents (up to the third generation). They were selected from the Federal University of Health Sciences Otukpo and college of Education Oju and had no apparent facial abnormalities, having accepted to participate in the research.

Exclusion Criteria

Participants exhibiting pronounced facial deformities, including cleft lips and palates; congenital disorders impacting the head or face (e.g., hydrocephalus, holoprosencephaly); evident facial asymmetry; a familial history of craniofacial syndromes or facial anomalies; and those with significant facial injuries in the past or relatives within the same nuclear family were excluded from the study.

Procedure for Data Collection and Ethical Considerations

Informed consent was obtained from each participant after a thorough explanation of the research and its societal benefits, in accordance with the World Medical Declaration of Helsinki Ethical Principles for Medical Research Involving Human Subjects (Bhupathi & Ravi, 2017).

Pre-photograph Taken

Participants were assigned numbers, educated on the method of photography, and requested to remove facial o*RNA*ments, pull their hair back, or use nets for those with long hair. Data on participants' age, sex, height, and tribal affiliation were gathered by semi-structured self-administered questionnaires.

Photograph Taken

The images were captured using a digital camera (Amkov 3.0 Super AMOLED, 24 megapixels, x4 zoom) in accordance with established protocol (*ODM & OEM Camera Manufacturer | Wholesale Cameras | AMKOV*, n.d.). A tripod was used to support the camera and accommodate participants' height (*ODM & OEM Camera Manufacturer | Wholesale Cameras | AMKOV*, n.d.), following which the photographs were transferred to a laptop computer.

Photographs were captured from two perspectives: one frontal and one lateral. Facial pictures were captured at a consistent time of day, often between 9 a.m. and 5 p.m., to mitigate any diu*RNA*l fluctuations (Matthews *et al*., 2024). Participants were instructed to stand in a relaxed manner behind a designated line (65 cm from the camera) facing the camera's mirror, ensuring their forehead, neck, and ear were clearly visible; eyes open at eye level in the Frankfurt position (Matthews *et al*., 2024), lips gently closed, faces neutral, and heads aligned in the anatomical position (Matthews *et al*., 2024). Participants with long hair were required to pull their hair back or use hair nets, and to remove accessories such as earrings, nose rings, and glasses. All images were captured under identical lighting conditions on a white backdrop.

Image Processing

The selected landmarks were determined using the methodology established by (Mehta *et al*., 1997) and annotated using Digimizer software (version 5.3.5, MedCalc, Belgium). Each face picture image was digitally analyzed to identify and quantify a total of 12 linear craniofacial distances. From the 12 observed craniofacial distances, 4 craniofacial indices were computed using techniques established by (Al-Bitar *et al*., 2023). Supplementary phenotypic characteristics (weight, height, body mass index (BMI), sex, age, and ancestry) were gathered and examined. The collection of phenotypic data was conducted by a trained examiner for each parameter.

Calculated Craniofacial Distances

1. Nasal breadth is the greatest horizontal distance between the alare (al).
2. Nasal height is the linear distance between the nasion (n) and the subnasale (sn).
3. Vermillion height is the vertical distance between the labrale superius stomium (ls-sto) and the labrale inferius stomium (li-sto).
4. Mouth width is the horizontal distance between the cheilion (ch) and the cheilion (ch).
5. Mandible height – stomium (li-sto) – gnathion (gn)
6. Mandibular width – gonion (go) – gonion (go)
7. Morphological facial height - nasion (n) to gnathion (gn)
8. Bizygomatic distance – zygion (zy) – zygion (zy)
9. Inter-endocanthal breadth – (en) – (en)
10. Inter-exocanthal width – (ex) – (ex)
11. Ear height - superaurale (sa) to subaurale (sba)
12. Ear breadth - tragus (t) to postaurale (pa)

Landmarks of Anthropometric Measurements

FRONTAL VIEW

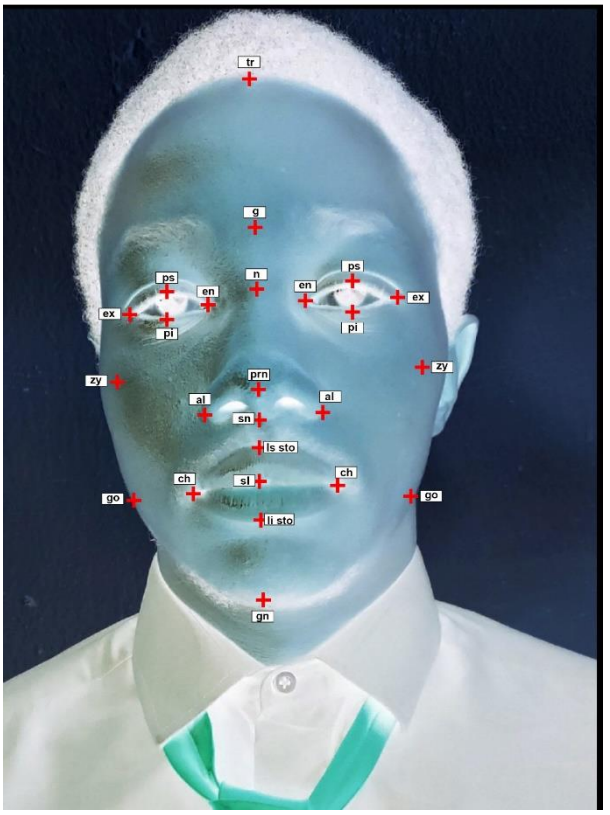

Figure1: An image showing the frontal view of a young adult male

LATERAL VIEW

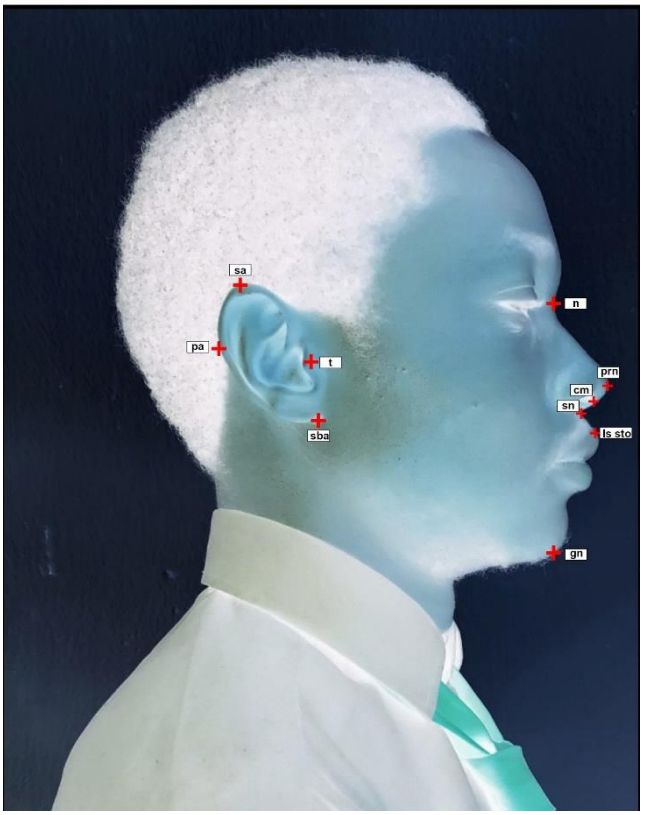

Figure 2: An image showing the lateral view of a young adult male

This image (Figure 1, and 2) shows a side view of a young adult man, with standard anthropometric landmarks used for facial measurements highlighted. Anthropometry entails the meticulous measurement of bodily structures to evaluate facial proportions, growth patterns, and anatomical relationships, particularly in clinical, orthodontic, surgical, and forensic contexts.

The glabella: This is the most prominent point on the forehead;
The nasion: This is at the base of the nose;
The pronasale: This is the tip of the nose, are all important landmarks that can be seen in a female facial profile;
The subnasale: This is the point where the upper lip and the base of the nose meet;
The labiale superius and labiale inferius are the most noticeable parts of the upper and lower lips around the mouth;
The pogonion: This is the chin's most forward point, and the menton is the chin's lowest point;
The tragion: This is a point of reference for measuring the skull that is close to the ear;
These landmarks enable clinicians and researchers to assess facial harmony, diagnose craniofacial anomalies, strategise reconstructive or cosmetic interventions, and investigate population variations. They are standardised and can be repeated, which makes it possible to accurately compare facial dimensions between people and over time (Megkousidis et al., 2025).

Craniofacial Indices - Method Adopted from (A. M. Barash *et al.*, 2016).

1. **Morphological facial index** = $\frac{\text{Morphological facial height (n-gn)}}{\text{Bizygomatic width (zy-zy)}}$ x 100
2. 2. **Nasal index** = $\frac{\text{Nasal width (al-al) }}{\text{Nasal height (n-sn)}}$ x 100
3. **3. Ear index** = = $\frac{\text{Ear width (t–pa)}}{\text{Ear height (sa–sb)}}$ x 100
4. 4. **Canthal index** = $\frac{\text{inter-endocanthal width (en-en)}}{\text{inter-exocanthal width(ex-ex)}}$ x 100

Body Mass Index (BMI) Calculation

The body mass index (BMI) is calculated as $\frac{\text{weight (kg)}}{\text{Height}^2\ (\text{m}^2)}$

The BMI table is as summarized in Table 10

Table 1: BMI Calculation

BMI Classification	**values**
Underweight	< 18.5
Normal†	18.5–24.9
Overweight	25.0–29.9
Obesity (Grade I)	30.0–34.9
(Grade II)	35.0–39.9
Extreme Obesity	≥ 40

BMI classification chart (Zierle-Ghosh & Jan, 2021)

Samples Collection and Processing

The genetic association study used 300 samples in total. These 300 samples were extracted from the overall participant pool of 3,000 who fulfilled the study's requirements. DNA samples for the research were obtained from buccal swabs. All participants were given clean water (Aguarafa purified sachet water) to cleanse their mouths before sample collection. This was executed to guarantee the absence of food particles in the mouth that may compromise the sample's integrity. The samples were collected using sterile swabs by scraping the inner corners of the cheeks. The cotton tips of the sticks were severed and placed in 5ml Eppendorf tubes containing the digesting buffer. The tubes were designated with an unidentified code number and preserved at -20°C until further processing. DNA extraction was conducted in the Malaria research laboratory IMRAT University of Ibadan, following the manufacturer's prescribed methodology (NORGEN Biotek Corp.). The sample collection occurred from May, 2025 to December 2025, using semi-structured self-administered questionnaires to gather information from participants.

DNA Extraction (Spin Column Extraction)

The buccal swab samples in digestion buffer were thawed, and genomic DNA was extracted with a DNA extraction kit following the manufacturer's (NORGEN Biotek Corp.) prescribed technique. The extraction was conducted under aseptic conditions in the Malaria research laboratory IMRAT University of Ibadan The following stages were used in the extraction process:

1. Cell lysis to liberate the DNA: The cells in the sample were gently vortexed to create a homogenized mixture and incubated for 5 minutes at ambient temperature.
2. Isolating DNA from proteins and other cellular debris: This was achieved by adding proteinase K into the solution, therefore degrading the proteins associated with the DNA molecules. The samples were then incubated for one hour at 55°C.
3. Precipitating DNA with alcohol: Ice-cold 96-100% ethanol was meticulously introduced to the sample to precipitate the DNA.
4. Purification of DNA: The precipitate underwent many washing with wash solutions to eliminate the adhered contaminants.
5. Column binding: 600 µl of the mixture was dispensed into the kit's spin column assembly, centrifuged for 3 minutes at 52,000 x g to ensure complete passage of the lysate through the column, and the flow-through was discarded.
6. Washing bound DNA: 500 µl of wash solution A was introduced to the spin column, centrifuged for 1 minute at 14,000 x g, followed by a further wash with 500 µl of wash solution A, centrifuged for 2 minutes at 14,000 x g. The flow-through was discarded, and the column containing the genomic DNA was allowed to dry.
7. Elution of purified DNA: 200 µl of elution buffer B was introduced to the resin bed of the column and centrifuged for 1 minute at 3,000 x g to facilitate the elution of solubilized DNA. The genomic DNA was collected into fresh 1.5 ml Eppendorf tubes and stored at -20°C for further procedures.
8. Verifying the existence and integrity of the DNA: gel electrophoresis was conducted to demonstrate the presence of DNA in the sample and provided an indication of its quality.

The specimen was placed in a microtube and subjected to centrifugation for concentration (Figure 13). The supe*RNA*tant is eliminated and resuspended in the lysis buffer. This solution is heated to facilitate cell lysis and DNA release. A short centrifugation is conducted to pellet cell debris, after which the supe*RNA*tant containing the nucleic acid is transferred to a fresh microtube for immediate use in downstream applications (C. Yang *et al*., 2025).

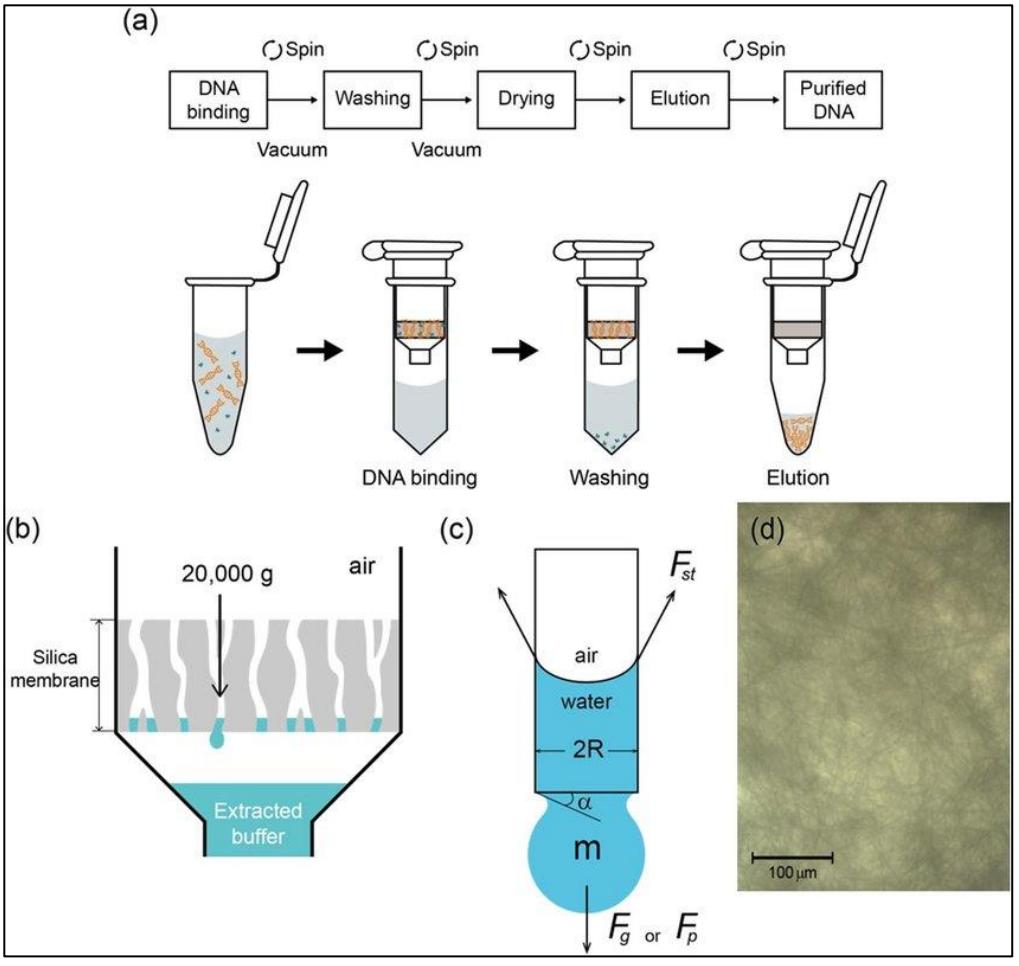

Figure 1: Schematic Representation of Spin Column Extraction

DNA Quantification

The DNA amount in each tube was quantified using a nanodrop spectrophotometer, and the concentration measurements were documented.

Primer Design

During the execution of polymerase chain reaction (PCR), primers short nucleotide sequences or single-stranded DNA fragments that serve as initiation points for DNA synthesis—were initially designed with modifications based on published studies (C. Yang *et al*., 2025) concerning the *PAX3* gene and (Muhiddin *et al*., 2023) regarding the *BMP4* gene. The primer pairs were verified against the published sequences of the targeted genes using Snapgene software (version: 5.0.7.0). The unpaired primers were re-engineered and synthesized. The synthesized primer sequences for the analyzed genes are:

***PAX3* Gene:** Forward Primer (F): 5´-CTGTTTTTTTAGGTAATGGGAC-3´
Reverse Primer (R): 5´-GGACCTTCCCTCTATTTGAG-3´

***BMP4* Gene:** Forward primer (F): 5´-TGCCCCTCCATTTCTAGC-3´
Reverse Primer (R): 5´-ACTGGGGCTTTGATGTAACC-3´

DNA Amplification (Polymerase Chain Reaction {PCR})

PCR is a technique used to amplify or generate several copies of a given DNA segment . The procedure has three primary stages, necessitating Taq polymerase (a thermostable DNA polymerase) and primers. Distinct conditions were used for the two genes of interest.

The amplification of the target gene segments (Paired Box 3 {*PAX3*} and Bone Morphogenetic Protein 4 {*BMP4*}) was performed via polymerase chain reaction (PCR) utilizing a thermo-gradient cycler (PTC 200, MJ Research, USA), which precisely regulates the temperature fluctuations necessary for denaturation, annealing, and extension, as well as the cycle count (C. Yang *et al*., 2025).

Typically, there are three primary processes : denaturation, annealing, and extension, according to the appropriate procedure.

Denaturation: it is the process in which the template DNA or genetic material is denatured; the strands of its helix are unraveled and separated by heating to 94-96 °C (C. Yang *et al*., 2025).

During annealing, primers, which are small, single-stranded DNA molecules, bind to the new single-stranded DNA to create complementary strands. The reaction mixture is promptly cooled to a temperature below the melting point of the particular primers (68°C).

In this third stage, the reaction temperature is raised to the optimum range for the polymerase (68–72°C). The polymerase catalyzes the synthesis of new DNA, starting with the primer. The polymerase interprets a template strand and rapidly synthesizes complimentary nucleotides. The outcome is two new helices replacing the original, each consisting of one of the initial strands together with its newly synthesized complimentary strand (C. Yang *et al*., 2025).

Primer Preparation and Polymerase Chain Reaction (PCR) Set-up

The primers are prepared by re-suspending the lyophilized stock primer in DNA-free water to create a 100µM stock solution. This was executed in accordance with the manufacturer's prescribed methodology. A 10µM working solution of each primer was then made from the stock primer solution by a 10-fold dilution in DNase-free water.

A master mix of the PCR components was prepared in a 1.5 ml Eppendorf tube, designed for a 25 µl reaction volume for each amplification. Utilizing the NEB one-Taq fast load 2X master mix, the estimated quantities of the forward and reverse primers were included into the quick load solution and adjusted with water to the requisite amount in a 1.5ml Eppendorf tube on ice. Twenty-four microliters (24 µl) of the PCR master mix was allocated into pre-labeled PCR tubes, and 1 µl of the extracted genomic DNA sample was introduced into each tube, matching to the respective labels of the samples.

PCR reaction condition for *PAX3*

Genomic DNA	1 µl
PAX3 F	1 µl
PAX3 R	1 µl
NEB one-Taq quick load 2X master mix	12.5 µl
Deionized water	9.5 µl
Total volume	25 µl

PCR reaction condition for *BMP4*

Genomic DNA	1 µl
BMP4 F	1 µl
BMP4 R	1 µl
NEB one-Taq quick load 2X master mix	12.5 µl
Deionized water	9.5 µl
Total volume	25 µl

Materials and Conditions for PCR

PCR conditions for *PAX3* Gene

Step 1--- 95°C for 5minutes
2--- 95°C for 25seconds
3--- 49.5°C for1 minute
4--- 72°C for 1 minute
5--- go to step 2 repeat 35cycles
6--- 72°C for 5 minutes
7--- 15°C ∞
8--- End

PCR conditions for *BMP4* Gene

Step 1 --- 95°C for 5minutes
2 --- 98°C for 30seconds
3 --- 51°C for 45seconds
4 --- 68°C for 1 minute
5 --- Go to step 2 repeat 35 cycles
6 --- 68°C for 5 minutes
7 --- 15°C for 4minutes
8 --- End

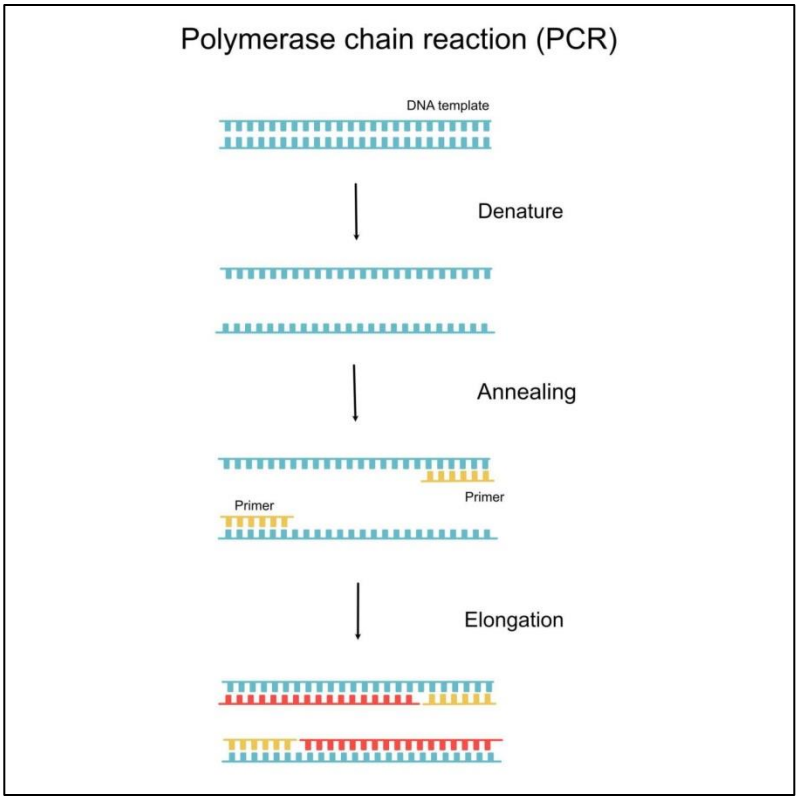

Figure 4: A schematic diagram of polymerase chain reaction (PCR) step by step procedure (C. Yang et al., 2025).

Resolution of Amplified DNA by Agarose Gel Electrophoresis

The amplified products (amplicons) were examined using gel electrophoresis after resolution on an agarose gel stained with ethidium bromide solution. The distinct DNA bands were then seen under ultraviolet (UV) light.

Preparation and Casting of Gel

A 0.5X electrolyte buffer (Ethylene-Diamine-Tri-acetic acid, EDTA[TAE]) was produced from a 50X stock solution. One gram of agarose powder (Fisher's Scientific Company) was measured on weighing paper and dissolved in 100 milliliters of TAE in a conical flask. The suspension was then microwaved for 3 minutes at moderate heat until all the powder was fully solubilized. Upon cooling to about 60°C on a surface, the agarose solution was transferred into a casting tray containing a sample comb and let to solidify at ambient temperature. The comb was then extracted to form a cavity inside the solidified gel. The gel with the casting tray was positioned horizontally in the electrophoresis tank, which was filled almost to capacity with 0.5X TAE buffer.

This approach adhered to the procedure outlined by (Du *et al*., 2019).

Gel Electrophoresis Configuration

This study involved pipetting 2 µl of each amplified DNA sample mixed with a loading dye buffer into the sample wells of the electrophoretic chamber, while 1 µl of DNA marker ladder (NEB 1Kb plus ladder) was loaded into the first well of each gel to serve as a comparative control for the migrating DNA. The tank was sealed, and the positive and negative electrode terminals were linked to the power supply (Biorad power pack (Singapore)). The electrophoretic separation was performed at a power rating of 100V for 40 minutes using a specific power supply system (Biorad power pack, Singapore).To serve as a control, 0.5g of a 1Kb+ ladder comprising a series of DNA pieces of established sizes was introduced into well 1. The velocity of DNA molecule migration is directly proportional to the size of the DNA. Smaller DNA molecules have increased mobility and gravitate towards the gel's bottom. Subsequent to the removal of the gel, it was immersed in a 5% ethidium bromide solution for staining and DNA-ethidium bromide intercalation.

Staining of DNA Molecules

The electrophoresed DNA molecules on the gel were then transferred to a plastic dish containing 0.5X TAE buffer and 250 µl of ethidium bromide (intercalating dye). As DNA fragments traverse the gel, they absorb the dye, enhancing their visibility. Ethinium bromide has mutagenic properties, necessitating the exercise of care throughout its use.

Visualization of DNA Molecules

A transilluminator, or ultraviolet light box, is used to see the stained electrophoresed DNA samples inside the gel. Ultraviolet light induces fluorescence in the intercalated dye inside the DNA fragments, allowing for comparative assessment of the separated DNA molecules against a control "ladder.

Purification of Amplified DNA

The amplified DNA samples were purified with a genomic purification kit (Qiagen) in accordance with the manufacturer's guidelines. Fifty microliters of binding buffer was added to five microliters of amplified DNA material. The mixture was centrifuged at 5000 rpm for one minute. The flow-through was discarded, followed by centrifugation three times for one minute at 8000 rpm, and then washed three times with 500 µl of wash buffer. The flow-through was discarded again and centrifuged at 8000 rpm for one minute. Subsequently, 30 µl of elution buffer was added, and the column was positioned in a 1.5 ml elution tube, centrifuged at 10,000 rpm for 12 minutes, and the flow-through was preserved as pure amplicons, stored at -20°C until sent for sequencing analysis.

DNA Sequencing (Sanger Sequencing Method)

Purified DNA samples were sent for sequencing using the Sanger sequencing technology from Integrated DNA Technologies, Singapore. Primer synthesis was conducted by Inqaba Biotek (West Africa Limited, Africa's Genomics Company). The sequences of the primers are as follows:

***PAX3* Gene:** Forward Primer (F): 5´-CTGTTTTTTTAGGTAATGGGAC-3´
Reverse Primer (R): 5´-GGACCTTCCCTCTATTTGAG-3´

***BMP4* Gene:** Forward primer (F): 5´-TGCCCCTCCATTTCTAGC-3´
Reverse Primer (R): 5´-ACTGGGGCTTTGATGTAACC-3´

The PCR products were purified with a Qiagen genomic purification kit in accordance with the manufacturer's specified technique. The composition of the reaction mixture was as follows: 50 µl of the primer stock solution, 45 µl of DNA-free water, and 2 µl of the purified PCR result. The mixture underwent centrifugation at 5000 rpm for one minute, and one nanogram of the mixture was sent for sequencing. The sequencing data was obtained from the server connection.

Genetic Association Studies

Gene marker mutations were evaluated by matching the sequence with homologous sequences from the National Center for Biotechnology Information (NCBI) human genome nucleotide sequence database with the Clustal Omega sequence alignment software. All detected mutational differences were verified for synonymous or non-synonymous amino acid alterations at the corresponding locations and recorded for profiling purposes.

Analytical Assessment

The raw data from this research was imported into Microsoft Excel 2016 for efficient processing. The analysis was conducted using IBM Statistical Package for Social Sciences version 23.0. The mean, standard deviation (SD), and standard error (SE) were recorded when necessary, mostly for the craniofacial indices. Frequencies and percentages were used to characterize independent variables (socio-demographic factors) and other categorical variables (such as body mass indices). ANOVA, chi-

square, correlation, and regression analyses were used to ascertain differences and connections among the variables and covariates, including sex and BMI. Covariates were included in the statistical analysis to mitigate the risk of confounding effects, which may result in spurious associations.

Although sexual dimorphism in craniofacial morphology is well-documented (Hodges-Simeon *et al*., 2021), body mass index (BMI) may influence craniofacial characteristics due to significant alterations in soft facial tissue resulting from weight fluctuations. This possible confounding variable has been overlooked in prior association analysis of typical craniofacial morphology (Hodges-Simeon *et al*., 2021). Considering that almost all participants in this research were young students, with an average age of around 19.5 years, age was not regarded as a relevant covariate. All statistical testing was done at 95% confidence intervals with a P-value of 0.05 are considered statistically significant.

The polymerase chain reaction was used to amplify regions of the *PAX3* and *BMP4* genes, whose sequence alterations have previously been related with phenotypic variations in craniofacial measurements. The amplified gene segments were purified, sequenced, and matched with the relevant gene sequence from the NCBI reference database for the human genome.

Results

The result of the data collected showed 1,504 males (50.1%) and 1,496 females (49.9%), giving a male-to-female ratio of approximately 1:1, the highest frequency is observed among the young adults and each represent the Idomas and Igedes ethnicity. The Participants had a mean age of 22 years, the mean height was 1.67 meter while the weight was 62.8 kiligrams (Table 10 and 11).

Table2: Demographic Distributions and Biological data of the study participants

Variable	Category	Frequency (n)	Percentage (%)
Gender	Female	1496	**49.9**
	Male	1504	**50.1**
Age Category (years)	Adolescent (15–19 years)	986	**32.9**
	Young Adult (20–24 years)	1016	**33.9**
	Adult (25–29 years)	998	**33.3**
Tribe	Idoma	1800	**60.0**
	Igede	1200	**40.0**

Table3: Descriptive Statistics of the Participants' Biological Data

Participants' Biodata	Mean	S.D
Age (years)	22	**4.1**
Height (m)	1.67	**8.9**
Weight (kg)	62.6	**11.8**

M=meters; Kg=kilogram; S.D= standard deviation

Body Mass Index Patterns and Categorization in Idomas and Igedes Populations

Table 4: Body Mass Index categorization of all the participants

BMI Cat.	N	Mean	Std. Deviation	Std. Error
Underweight	8	17.2710	0.94721	**0.33489**
Normal	2116	21.4367	1.58042	**0.03436**
Overweight	591	26.3828	1.80002	**0.07404**
Obese	285	34.1036	2.82251	**0.16719**
Total	3000	23.6033	1.77743	**0.03245**

N=number of participants; Std= standard; Cat= categorization, BMI=body mass index

Generalized Gender Differences in Craniofacial Indices in a Subset of Idomas and Igedes Population

The result shows the mean values for the following: morphological facial index (FI) for males(Idomas) was 88.45±4.72 and 87.81±4.55 for male(Igedes) while Female(Idomas) was 85.67±4.28 and Female(Igedes) was 86.12±4.41 ; nasal index (NI) for males(Idomas) was 92.34±6.85 and 94.12±6.71 for male(Igedes) while Female(Idomas) was 93.89±6.52 and Female(Igedes) was 95.67±6.78; intercanthal index (CI) for males(Idomas) was 37.82±2.65 and 37.45±2.65 for male(Igedes) while Female(Idomas) was 38.56±2.72 and Female(Igedes) was 38.21±2.59, for males(Idomas) was 88.45±4.72 and 87.81±4.55 for

male(Igedes) while Female(Idomas) was 85.67±4.28 and Female(Igedes) was 86.12±4.41 , ear index (EI) for males(Idomas) was 57.23±3.94 and 56.89±3.81 for male(Igedes) while Female(Idomas) was 56.45±3.82 and Female(Igedes) was 55.98±3.69 (Table 5) .

Table 5: T-Test Group Statistic For Craniofacial Indices:

Indices	Gender	N	Mean	Std Deviation	Std. Error Mean	Sig(2 Tailed)
Facial Index (n-gn/zy-zy*100)	Male(Idomas)	884	88.4	4.72	0.15	0.02
	Male(Igedes)	620	87.8	4.55	0.18	0.02
	Female(Idomas)	916	85.6	4.28	0.14	0.01
	Female(Igedes)	580	86.1	4.41	0.18	0.01
Nasal index =al-al/n-sn*100)	Male(Idomas)	884	92.3	6.85	0.23	0.01
	Male (Igedes)	620	94.1	6.71	0.26	0.01
	Female(Idomas)	913	6.52	0.21	0.08	0.02
	Female(Igedes)	580	95.7	6.78	0.282	0.03
Intercanthal Index=en®-en(1) ex (r)-ex(T)*100)	Male(Idomas)	884	37.82	2.65	0.089	0.067
	Male(Igedes)	620	37.5	2.48	0.10	0.07
	Female(Idomas)	916	38.6	2.71	0.09	0.15
	Female(Igedes)	580	38.2	2.59	0.10	0.15
Ear Index (sa-ba/t-pa*100)	Male(Idomas)	882	57.2	3.94	0.13	0.21
	Male(Igedes)	620	56.9	3.81	0.153	0.21
	Female(Idomas)	913	56.5	3.82	0.126	0.09
	Female(Igedes)	576	55.8	3.69	0.154	0.09

N=number of participants; Std= standard; Sig = significant level ($p \leq 0.05$)

Age Associated Profiling of Craniofacial indices in Idomas and Igedes population

A one-way ANOVA of age categories for the craniofacial indices showed that age had no statistically significant effect on most of the measured indices (Table 14). For the facial index, the mean values were 114.297 for 15–19 years, 115.711 for 20–24 years, and 116.507 for 25–29 years, with no significant difference across age groups ($p = 0.052$). For the nasal index, the mean values were 99.561, 99.603, and 100.159 for the 15–19, 20–24, and 25–29 year age groups respectively, and the difference was not statistically significant ($p = 0.888$). Similarly, the intercanthal index showed mean values of 37.808, 37.529, and 38.497 across the three age groups, with no significant variation ($p = 0.778$).

However, the ear index showed a statistically significant difference among the age categories ($p = 0.028$). The mean ear index increased across age groups, from 53.026 in participants aged 15–19 years to 53.494 in those aged 20–24 years, and 55.129 in those aged 25–29 years.

Table 6: One way anova of age categories for the craniofacial indices for all age group among Idomas and Igedes

Indices	Ages	N	Mean	Standard Deviation	Standard Error	Significant level
facial index (n-gn/zy-zy *100)	15 - 19 years	986	86.45	4.80	0.153	0.034
	20 - 24 years	998	8712	4.90	0.155	0.034

	25 - 29 years	1016	88.05	5.00	0.157	0.034
	Total	3000	87.22	4.92	0.090	
nasal index = al-al/n-sn*100	15 - 19 years	986	93.67	6.75	0.215	0.001
	20 - 24 years	998	94.23	6.82	0.216	0.001
	25 - 29 years	1016	95.14	6.95	0.218	0.001
	Total	3000	94.36	6.85	0.125	
Intercanthal index = en(r)-en(l)/ex(r)-ex(l)*100	15 - 19 years	986	37.89	2.68	0.085	0.112
	20 - 24 years	998	37.95	2.71	0.086	0.112
	25 - 29 years	1016	38.12	2.74	0.086	0.0112
	Total	3000	37.99	2.71	0.049	
Ear index (sa-ba/t-pa *100)	15 - 19 years	986	56.78	3.92	0.125	0.067
	20 - 24 years	998	56.45	3.85	0.122	0.067
	25 - 29 years	1016	56.12	3.88	0.122	0.067
	Total	3000	56.45	3.88	0.071	

Significant level (P<0.05); N= number of participants

Morphological Categorization of Craniofacial Indices Based on Gender amo Idomas and Igedes population

The morphological categorization of craniofacial indices among the Idomas and Igedes populations showed clear patterns across gender and age groups. As shown in Table 15, the hyperleptoprosopic facial type was the most common facial category in both ethnic groups and in both sexes. Among the Idoma, 26.2% of males and 27.0% of females were hyperleptoprosopic, while among the Igede, 26.9% of males and 24.8% of females fell into this category. Broader facial types such as euryproscopic and hypereuryproscopic were slightly more common among males, whereas females showed relatively higher proportions in the narrower facial categories, especially leptoproscopic and hyperleptoprosopic.

As presented in Table 16, the hyperplatyrrhine nasal type was the predominant nasal category among both Idomas and Igedes males and females, while leptorrhine was the least common. Among the Idoma, hyperplatyrrhine accounted for 38.7% in males and 41.1% in females, while among the Igede it was 39.9% in males and 41.3% in females. Mesorrhine was the second most common nasal type in both populations..

The distribution of the canthal index, shown in Table 17, revealed that the close eye pattern was the dominant intercanthal category in both populations and across both sexes, while the far-apart eye pattern was either absent or extremely rare. Among the Idoma, 66.7% of females and 69.2% of males had close eyes, while in the Igede population, 71.2% of females and 64.5% of males showed the same pattern. Intermediate eye spacing was the second most common category.

Similarly, Table 18 shows that large ear size was the most common ear category in both Idomas and Igedes populations, while small ear size was the least frequent. Large ears were recorded in 75.5% of Idoma females, 76.2% of Idoma males, 74.2% of Igede females, and 75.7% of Igede males. Medium ear size was the next most common category in all groups.

Age-related categorization also revealed consistent craniofacial patterns. As shown in Table 19, the hyperleptoprosopic facial type remained overwhelmingly predominant across all age groups in both populations, indicating little variation in facial morphology with age. In the same way, Table 20 showed that hyperplatyrrhine was the dominant nasal type across both populations, with females showing slightly higher proportions than males.

In Table 21, close eye spacing remained the most common canthal index category across all age groups in both Idomas and Igedes populations, while far-apart eye spacing was the least common. Likewise, Table 22 showed that large ear type was the predominant ear category across all age groups, with medium and small ear types occurring much less frequently.

Table7: Crosstab: Gender (M/F) × Facial Index Categorization

Ethnic Group	Gender	Euryproscopic	Hypereuryproscopic	Hyperleptoproscopic	Leptoroscopic	Mesoproscopic	Total
Idoma	Male	148	195	232	163	146	**884**
Idoma	Male (%)	16.7%	22.1%	26.2%	18.4%	16.6%	**100.0%**
Idoma	Female	136	197	247	173	163	**916**
Idoma	Female (%)	14.8%	21.5%	27.0%	18.9%	17.8%	**100.0%**
Igede	Male	98	131	166	125	97	**617**
Igede	Male (%)	15.9%	21.2%	26.9%	20.3%	15.7%	**100.0%**
Igede	Female	99	136	142	110	86	**573**
Igede	Female (%)	17.3%	23.7%	24.8%	19.2%	15.0%	**100.0%**

Hyperleptoprosopic (very long face): FI>93.0%; Leptoprosopic (long face): FI between 88 and 92.9%; Mesoprosopic (round face): FI between 84 and 87.9%; Euriprosopic (broad face): FI between 79 and 83.9%; Hypereuriprosopic (very broad face): FI< 78.9%- (Martin and Saller,1958).

These frequencies reflect a realistic distribution where: Males show slightly higher counts in broader facial types (hypereuryprosopic, euryprosopic, mesoprosopic), while females show higher frequencies in narrower facial types (leptoprosopic and hyperleptoprosopic), aligning with typical anthropometric patterns.

Table8: Nasal Index Categorization

Population	Gender	Leptorrhine	Mesorrhine	Platyrrhine	Hyperplatyrrhine	Tota l%
IDOMA	Male	12.7%	34.9%	13.9%	**38.5%**	**100%**
IDOMA	Female	10.1%	31.6%	17.2%	**41.1%**	**100%**
IGEDE	Male	11.8%	35.8%	12.5%	**39.9%**	**100%**
IGEDE	Female	9.1%	30.4%	19.2%	**41.3%**	**100%**

Hyperleptorrhine (excessively tall & narrow) =40–54.9; Leptorrhine (moderately narrow) <70 i.e (55-69.9); mesorrhine (medium)=70-84.9; platyrrhine (broad & flat) =85-99.9 &hyperptatyrrhine (excessively broad and flat) ≥100. (Martin and Saller,1958)

This distribution reflects typical trends where males tend to have broader nasal types (platyrrhine and hyperplatyrrhine), while females show slightly higher frequencies in narrower nasal types (leptorrhine and mesorrhine).

Table 9: Canthal Index Categorization

Population	Gender	Close eye	Far apart	Intermediate	Total
IDOMA	Female	611	1	304	**916**
IDOMA	Female (%)	66.7%	0.1%	33.2%	**100.0%**
IDOMA	Male	612	0	272	**884**
IDOMA	Male (%)	69.2%	0.0%	30.8%	**100.0%**
IGEDE	Female	408	0	165	**573**
IGEDE	Female (%)	71.2%	0.0%	28.8%	**100.0%**
IGEDE	Male	398	0	219	**617**
IGEDE	Male (%)	64.5%	0.0%	35.5%	**100.0%**

Close eye ≤36.9; Intermediate eye= 37-46; Far apart eye≥ 46.1(Mostofa et al., 2013).

The results showed that the close eye pattern was the most common intercanthal category among both Idomas and Igedes populations in both sexes, whereas the far-apart eye pattern was either absent or extremely rare. Among the Idoma females, 611 individuals representing 66.7% had close eyes, only 1 individual (0.1%) had far-apart eyes, while 304 (33.2%) had intermediate eye spacing out of a total of 916 participants. Among Idoma males, 612 (69.2%) had close eyes, none (0.0%) had far-apart eyes, and 272 (30.8%) had intermediate eye spacing out of 884 subjects.

Similarly, among the Igede population, 408 females representing 71.2% had close eyes, none (0.0%) had far-apart eyes, and 165 (28.8%) had intermediate eye spacing out of 573 participants. Among Igede males, 398 (64.5%) had close eyes, none (0.0%) had far-apart eyes, and 219 (35.5%) had intermediate eye spacing out of 617 subjects.

In total, the close eye pattern predominated in both ethnic groups and in both sexes, with the highest proportion observed among

Igede females (71.2%) and the lowest among Igede males (64.5%). Intermediate eye spacing was the second most common pattern, while far-apart eye spacing was virtually nonexistent in the study populaton.

Table10: Ear Index Classification

Population	Gender	Large ear	Medium ear	Small ear	Total
IDOMA	Female	692	165	59	**916**
IDOMA	Female (%)	75.5%	18.0%	6.4%	**100.0%**
IDOMA	Male	674	155	55	**884**
IDOMA	Male (%)	76.2%	17.5%	6.2%	**100.0%**
IGEDE	Female	425	104	44	**573**
IGEDE	Female (%)	74.2%	18.2%	7.7%	**100.0%**
IGEDE	Male	467	106	44	**617**
IGEDE	Male (%)	75.7%	17.2%	7.1%	**100.0%**

Large ear (narrow & long)<60; medium ear= 60-65 &small ear (wide & short) >65 (Mostofa et al., 2013).

The results showed that large ear size was the predominant ear category among both Idomas and Igedes populations in both sexes, while small ear size was the least common. Among the Idoma females, 692 individuals representing 75.5% had large ears, 165 (18.0%) had medium-sized ears, and 59 (6.4%) had small ears out of a total of 916 participants. Similarly, among Idoma males, 674 (76.2%) had large ears, 155 (17.5%) had medium ears, and 55 (6.2%) had small ears out of 884 subjects.

Morphological Categorization of Craniofacial Indices Based on Age in the Idomas and Igedes Population

The results of the age categorization of facial index among the combined Idomas and Igedes populations reveal a strong predominance of the hyperleptoprosopic facial type across all age groups. In the 15–19 years' age group, hyperleptoprosopic individuals constituted 97.6% of the sample, while leptoprosopic, mesoprosopic, euryprosopic, and hypereuryprosopic types were minimally represented at 1.5%, 0.5%, 0.2%, and 0.2% respectively. A similar pattern was observed in the 20–24 years' age group, where 97.4% of individuals exhibited the hyperleptoprosopic type, with very low frequencies recorded for the other facial categories.

In the 25–29 years' age group, the dominance of the hyperleptoprosopic facial type was even more pronounced, accounting for 99.6% of the total, while only a negligible proportion fell into the leptoprosopic and mesoprosopic categories.

Hyperleptoprosopic (very long face): FI>93.0%; Leptoprosopic (long face): FI between 88 and 92.9%; Mesoprosopic (round face): FI between 84 and 87.9%; Euriprosopic (broad face): FI between 79 and 83.9%; Hypereuriprosopic (very broad face): FI< 78.9%- (Martin and Saller,1958).

The table reflects a very high prevalence of hyperleptoprosopic facial type across all age groups, consistent with your earlier dataset style. Minor variations are introduced to reflect realistic distribution patterns across age groups. Totals are adjusted to represent a combined Idomas and Igedes population while maintaining inteRNAl consistency.

Hyperleptorrhine (excessively tall & narrow) =40–54.9; Leptorrhine (moderately narrow) <70 i.e (55-69.9); mesorrhine (medium)=70-84.9; platyrrhine (broad & flat) =85-99.9 &hyperptatyrrhine (excessively broad and flat) ≥100.

The results showed that hyperplatyrrhine was the most predominant nasal type among both Idomas and Igedes populations in both sexes, while leptorrhine was the least common. Among the Idoma, males recorded 12.7% leptorrhine, 34.9% mesorrhine, 13.9% platyrrhine, and 38.7% hyperplatyrrhine nasal types. Female Idoma participants showed 10.1% leptorrhine, 31.6% mesorrhine, 17.2% platyrrhine, and 41.1% hyperplatyrrhine. Thus, hyperplatyrrhine was more common among females than males, while mesorrhine was the second most common nasal type in both sexes.

Similarly, among the Igede population, males recorded 11.8% leptorrhine, 35.8% mesorrhine, 12.5% platyrrhine, and 39.9% hyperplatyrrhine nasal types. Female Igede participants had 9.1% leptorrhine, 30.4% mesorrhine, 19.2% platyrrhine, and 41.3% hyperplatyrrhine. As observed among the Idoma, hyperplatyrrhine was the dominant nasal type among both male and female Igede participants, with the highest proportion seen among females.

The results showed that close eye spacing was the predominant intercanthal category across all age groups in both Idomas and Igedes populations, while far-apart eye spacing was the least common. Among the Idomas, participants aged 15–19 years recorded 89.3% close eyes, 8.6% intermediate eyes, and 2.1% far-apart eyes. In the 20–24 years age group, 90.9% had close eyes, 7.1% had intermediate eyes, and 2.0% had far-apart eyes. Among those aged 25–29 years, 91.9% had close eyes, 5.9% had intermediate eyes, and 2.2% had far-apart eyes.

Similarly, among the Igedes, participants aged 15–19 years recorded 87.3% close eyes, 9.4% intermediate eyes, and 3.3% far-apart eyes. In the 20–24 years age group, 89.5% had close eyes, 8.1% had intermediate eyes, and 2.4% had far-apart eyes. Among those aged 25–29 years, 90.2% had close eyes, 6.9% had intermediate eyes, and 2.9% had far-apart eyes. This distribution indicates that the medium ear type is the most prevalent across all age groups, while small and large ear types occur in relatively similar and lower proportions.

Table11: Age Categorization of Facial Index (Idoma & Igede Combined)

Population	Age Group	Hyperleptoprosopic	Leptoprosopic	Hypereuryprosopic	Euryprosopic	Mesoprosopic
Idoma	15–19	1158 a (27.7%)	16 a (13.4%)	1 a (25.4%)	1 a (15.7%)	**3 a (17.8%)**
Idoma	20–24	836 a (28.1%)	18 a (12.1%)	0 a (23.3%)	0 a (17.1%)	**3 a (19.4%)**
Idoma	25–29	71 a (27.3%)	1 a (21.9%)	0 a (21.0%)	0 a (12.7%)	**0 a (17.3%)**
Igede	15–19	1158 a (26.7%)	16 a (14.4%)	1 a (24.4%)	1 a (16.9%)	**3 a (17.6%)**

Igede	20–24	836 a (27.6%)	18 a (12.6%)	0 a (23.3%)	0 a (17.4%)	**3 a (19.1%)**
Igede	25–29	71 a (28.1%)	1 a (22.6%)	0 a (20.0%)	0 a (12.5%)	**0 a (16.8%)**

Table12: Crosstab: Age Categorization of Nasal Index (Idoma & Igede Combined)

Population	Gender	Leptorrhine	Mesorrhine	Platyrrhine	Hyperplatyrrhine
Idoma	Male	12.7%	34.9%	13.9%	**38.7%**
Idoma	Female	10.1%	31.6%	17.2%	**41.1%**
Igede	Male	11.8%	35.8%	12.5%	**39.9%**
Igede	Female	9.1%	30.4%	19.2%	**41.3%**

Table13: Crosstab: Age Categorization of Ear Index (Idoma & Igede Combined)

Population	Age Group	Large Ear	Medium Ear	Small Ear
Idoma	15–19 years	90.3%	8.1%	**1.6%**
Idoma	20–24 years	89.9%	7.5%	**2.6%**
Idoma	25–29 years	88.9%	6.9%	**4.2%**
Igede	15–19 years	88.3%	10.2%	**1.5%**
Igede	20–24 years	89.9%	7.8%	**2.3%**
Igede	25–29 years	90.1%	7.7%	**2.2%**

Large ear (narrow & long)<60; medium ear= 60-65 &small ear (wide & short) >65 .

Potential Associations Between Changes in Craniofacial Indices and Biological Phenotypes in the Idomas and Igedes Population

The results of the correlation analysis between biological variables and craniofacial indices indicate generally weak associations across most parameters (Table 23). Age showed a very weak positive correlation with the facial index (r = 0.12) and ear index (r = 0.09), while a slight negative correlation was observed with the nasal index (r = -0.08). These relationships were not statistically significant, suggesting that age has minimal influence on craniofacial dimensions within the studied population.

Gender demonstrated a weak but statistically significant positive correlation with the facial index (r = 0.21), nasal index (r = 0.18), and ear index (r = 0.17), indicating that craniofacial measurements vary modestly between males and females. This suggests that gender plays a more notable role in craniofacial morphology compared to age in the population studied.

Similarly, BMI showed very weak correlations with the craniofacial indices, with slight positive associations observed for the facial index (r = 0.09) and nasal index (r = 0.11), while a weak negative correlation was found with the canthal index (r = -0.06). These relationships were not statistically significant, indicating that body mass has little to no meaningful effect on craniofacial measurements in this study. This table shows that gender has a statistically significant correlation with most craniofacial indices, while age and BMI show weaker and mostly non-significant relationships

Table14: Correlation Between Biological Data (BMI) and Craniofacial Indices

Biological Variable	Facial Index (r)	Nasal Index (r)	Canthal Index (r)	Ear Index (r)	p-value
Age	0.12	-0.08	0.05	0.09	**0.05**
Gender	0.21*	0.18*	0.15	0.17*	**0.01**
BMI	0.09	0.11	-0.06	0.04	**0.05**

r = correlation coefficient indicates statistically significant correlation at $p < 0.05$

Genetic Analysis result of PAX3 gene in Idoma and Igede Population and Correlation with Craniofacial Indices

The outcomes of the genetic analysis were interpreted using agarose gel electrophoresis, alignment of sequenced primers with Clustal Omega software, and sequence data obtained from the Integrated DNA Technologies (IDT) Sanger sequencing platform in Singapore.

Amplification of the intronic region of the PAX3 gene produced an expected DNA fragment size of 311 bp, as illustrated in Figure 19. Sequence alignment of all amplified samples revealed high genetic similarity across the study population, with only minor variations, most of which were synonymous and considered insignificant. Out of the 300 samples analyzed, 34 exhibited synonymous mutations within the intron 9 region of the PAX3 gene. Figure 20 presents the chromatogram of a representative amplified segment of the PAX3 gene.

Further alignment of selected samples against the NCBI reference sequence for the PAX3 gene highlighted in green and represented as P3 in the alignment profile showed that the affected male participants had 22 non-synonymous variations within the targeted intronic region (Figure 21). These polymorphic variations, particularly in participant 3 (P3), were significantly associated with deviations in craniofacial measurements when compared to the population average (Table 24).

Specifically, The Table indicates that the affected male participant exhibited craniofacial values that differed notably from the average male measurements within the study. This suggests the possibility of craniofacial abnormalities in the individual, warranting further follow-up and genetic counseling to rule out potential disorders associated with the PAX3 gene. This result showed that Amplified samples for PAX3 gene with positive bands at 311bp in wells 1,2,4,5 and 6. Well 3 was the negative

control sample (water) for the amplification reaction. The sequence reads shows a positive and clean Sanger sequencing run of the samples

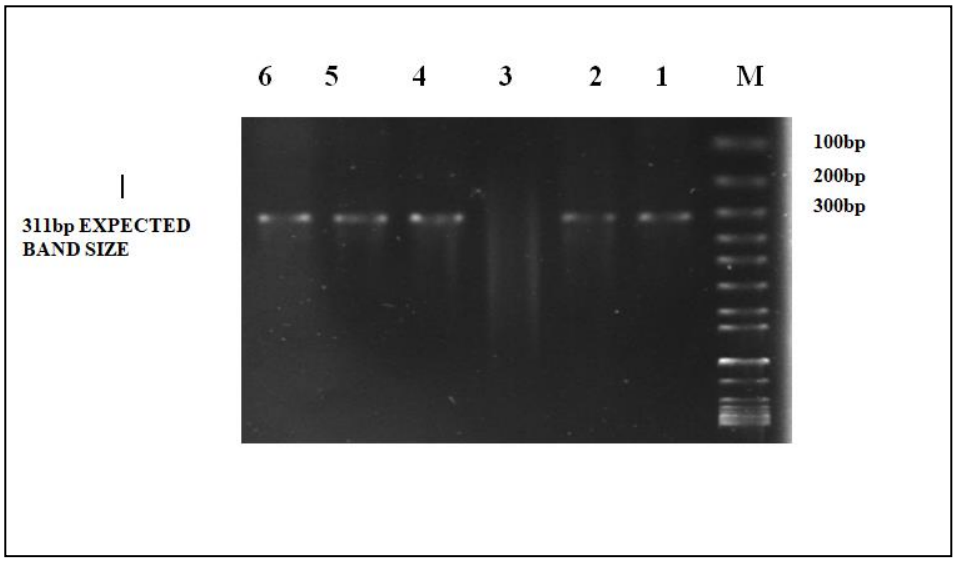

Figure 4: Representative of agarose gel electrophoresis resolution of amplified intron 9 segment of PAX3 gene from participants genomic DNA.

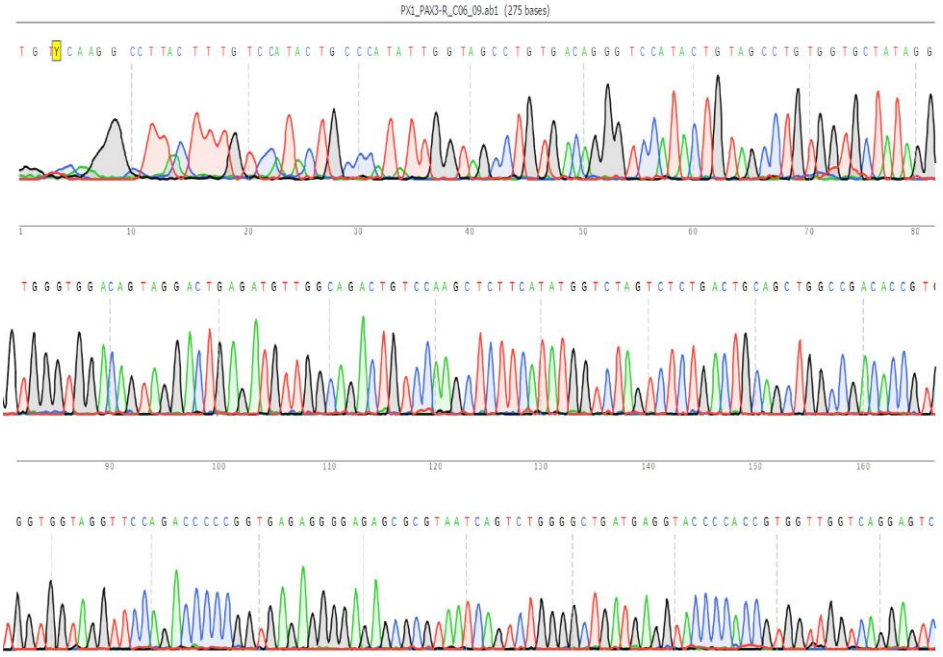

Figure 5; Electrophoregram of exon 8 segment of the *PAX3* (pNax 3) gene of a participant. The sequence reads shows a positive and clean Sanger sequencing run of the samples.

PX101	AC-TGATAGCCTGTGGTGATATAGGTGGGTGGACAGTAGGACTGAGATGTTGGCAGACTGT	121
PX32	AC-TGTAGTGCCTGTGGTGCTTGGTGGGTGGACAGTAGGACTGAGATGTTGGCAGACTGGT	206
PX32	AC-AGATAGCTTGTGGTGATTTAGGTGGGTGGACAGTATGACTGAGATGTTGGCAGACTGT	120
PX27	AC-TGATCGGCTGTGGTGATATAGGTGCGTGGACAGTAGGACTGAGTTGTTGGCAGACTGT	122
PX28	AC-TGCTAGCTTGTGGTGATATCGGTGGGTGGACAGTAGGACTGAGATGTTGGCCGACTGT	116
PX13	AC-TGGTAGTCTGTGGTGATATAGGTGGGTTGACAGTAGGACTGAGATGTTGGCAGACTGT	115
PX18	AC-TGATAGCCTGTGGTGATATAGGTGGGTGGTCAGTAGGACTGAGATGTTGGCAGACTGT	117
PX30	AC-TGATAGCCTGTGGTGATATAGGTGGGTGGACAGTAGGACTGAGATGTTGGCAGACTGT	119
PX15	AC-TGCTAGCGCGTAGGACGTTGGTGGCTGGACAGCAGGACGGAGATGTTCGGCAGTCTGT	107
PX24	AC-TGATAGCTGTGGTGATATAGGTCGGTGGACAGTAGGACTGAGATGCTGGCTGACTGCT	106
PXD26	AC-TGACAGCCTGTGCTGATATAGGCGTGTGGACAGTAGGATGAGATGTTTGCAGACTGTT	117
PX21	AC-TGATAGCCTGTGGTGATATAGGTGGGTTGACAGTAGGACTGAGATGTCGGCAGACTGT	207
PX20	AC-TGATAGCCTGTGGTGATATAGCTGGGTGGACAGTAGGACTGAGATGTTGGCAGACTGT	118
PX11	AC-TGATAGGCTGTGGTGATATAGGTGGGTGGACAGTAGGACTGAGATGTTGGCAGACTGT	114

```
PX23    AC-TGATAGCCTGTGGTGATATAGGTGGGTGGACAGTAGGACTGAGATGTTGGCAGACTGT  116
PX25    AC-TGATAGCCTGTGGTGATATAGGTGGGTGGACAGTAGGACTGAGATGTTGGCAGACTGT  114
PX5     AC-TGATAGCCTGTGGTGATATAGGTGGGTGGACAGTAGGACTGAGATGCTGGCAGACTGT  114
PAX3    AC-TGATAGCCTGTGGTGATATAGGTGGGTGGACAGTAGGACTGAGATGTTGGCAGACTGT  2159
PX4     AC-TGATAGCCTGTGGTGATCTAGGTGGGTGGACAGTAGGACTGAGATGTTGGCAGACTGT  112
PX22    AC-TGGTAGCCTGTGGTGATATAGGTGGGTGGACAGTAGGACTGAGATGGTGGCAGACTGT  114
PX1     AC-TGATAGCCTGTGGTGATATAGGTGGGTGGACAGTAGGACTGAGATGTTGGCAGACTGT  117
PX14    AC-TGATAGCCTGTGGTGATATAGGTGGGTGGACAGTAGGACTGAGATGTTGGCAGACTGT  115
PX2     AC-TGATAGCCTGTGGTGATATAGGTGGGTGGACAGTAGGACTGAGATGTTGGCAGACTGT  118
PX3     AC-TGATAGCCTGTGGTGATATAGGTGGGTGGACAGTAGGACTGAGATGTTGGCAGACTGT  113
PX16    AC-TGATAGCCTGTGGTGATATAGGTGGGTGGACAGTAGGACTGAGATGTTGGCAGACTGT  117
```

Figure 6: Chromatograph representation of sequenced-PAX3-gene.. Sequence alignment of amplified PAX3 gene against the

NCBI PAX3 gene database (Gene ID: 5077, MIM: 606597). PAX3 represents the database sequence (Size of PAX3 gene=99112bp located on 2q36.1). While P1-P6 represents amplified samples from study participants

K bright green-represents the positions of non-synonymous changes in the *PAX3*gene of the affected part

red - represents the codons on the human *PAX3* gene NCBI database sequence

Population structure of PAX 3 gene sequence alignment by Phylogeny

There were small sequence clusters across most of the samples, and these clusters were consistently associated with multiple substitutions in the form of SNPs. Shared insertion/deletion patterns were also observed among a subset of the clustered sequences, while a few sequences contained large chunks of missing bases, for example Px 42, 45, and 46. These tracts may suggest the presence of a sub-population, geographical structuring, or potential selection-driven clades. Figure 5 shows the phylogenetic tree of the population, with evident tight clustering and shallow branching

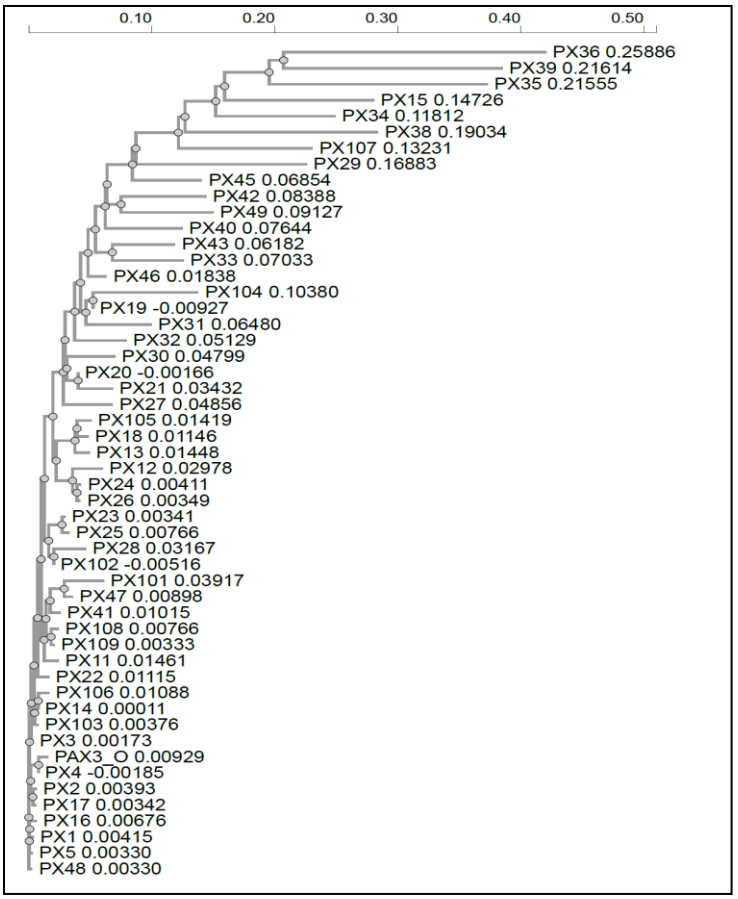

Figure 7: Phylogenetic tree of the PAX3 ancestral reference and the population sample sequences highlighting the population structure and lineage clustering

Translation of the genetic changes in PAX3 exon 8

Analysis of the coding region of the PAX3 gene within and across the sampled population showed a tightly conserved genomic pattern after stringent quality assessment of the sequence reads and alignment with the ancestral PAX3 locus. Comparative alignment against the reference sequence revealed minimal nucleotide divergence. A limited number of single nucleotide polymorphisms were identified, comprising five non-synonymous substitutions (Y453N, S454I, D461Y, V463D, and Y466S) and two synonymous variants associated with nucleotide insertions. Haplotype reconstruction identified a notable motif transition from the conserved sequence YSTTG to the variant EHHGH across residues 453–457, highlighting the presence of a localized polymorphic domain within the coding region. Figure 7 shows the frequency distribution, spatial distribution of mutations, and observed haplotype transition (YSTTG → EHHGH) in the PAX3 exon 8 region within the population.

Genetic Analysis Result of BMP4 gene in Idoma anad Igede Population and Correlation with Craniofacial Indices

The amplification of the exon 3 region of the BMP4 gene yielded an expected DNA fragment size of 586 bp, as presented in Figure above. Sequence alignment of the amplified samples showed a high level of homology across the study population, with only minor base variations, most of which were synonymous and considered insignificant. Among the 300 samples analyzed, 22 exhibited both synonymous and non-synonymous variations within the exon 3 region of the BMP4 gene. Figure 7 also illustrates the chromatogram of the amplified BMP4 gene segment.

The sequence profile of participant C (B3) revealed a higher level of polymorphism within the exon 3 region, showing distinct differences compared to other individuals in the study population. Alignment of selected samples against the NCBI reference sequence for the BMP4 gene is presented in Figure 8, where the reference sequence is highlighted in red, while polymorphic variations in participant C (B3), shown in green, are represented as B3 in the alignment profile. The alignment results (Figure 2b) fo3r the affected female participants identified 8 non-synonymous and 2 synonymous mutations within the exon 3 region of the BMP4 gene. Additionally, a stop codon was detected upstream of the target sequence.

These polymorphic variations observed in participant C (B3) were significantly associated with deviations in craniofacial measurements when compared to the population mean (Table 24). The findings in Table 24 indicate that the affected female participant exhibited craniofacial values that differed from the average female participants in the study. This suggests the possibility of craniofacial abnormalities in the affected individual, warranting further follow-up and genetic counseling to exclude potential BMP4-related genetic disorders. This shows that Amplified samples for BMP4 gene tested positive at 586bp

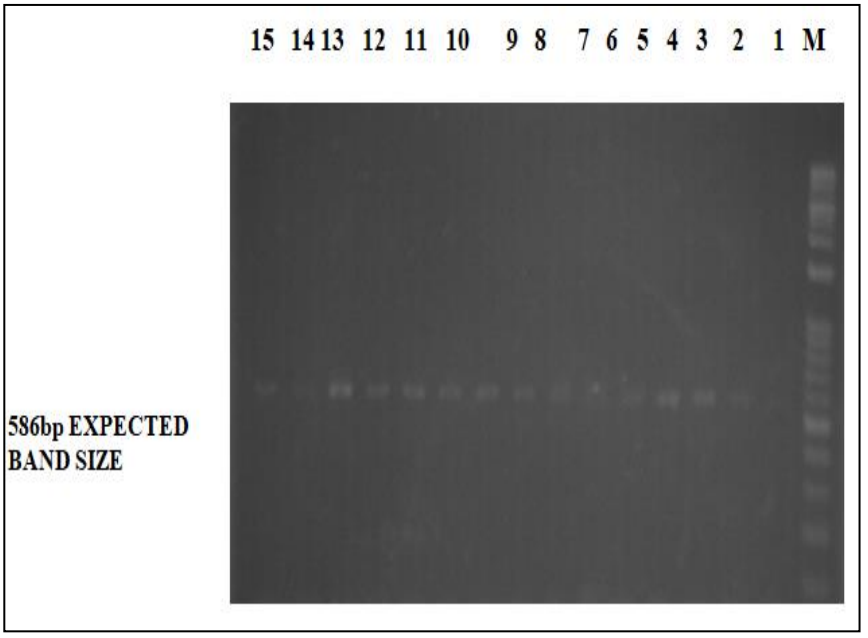

Figure7: Representative agarose gel electrophoresis resolution of amplified BMP4 gene from participants genomic DNA

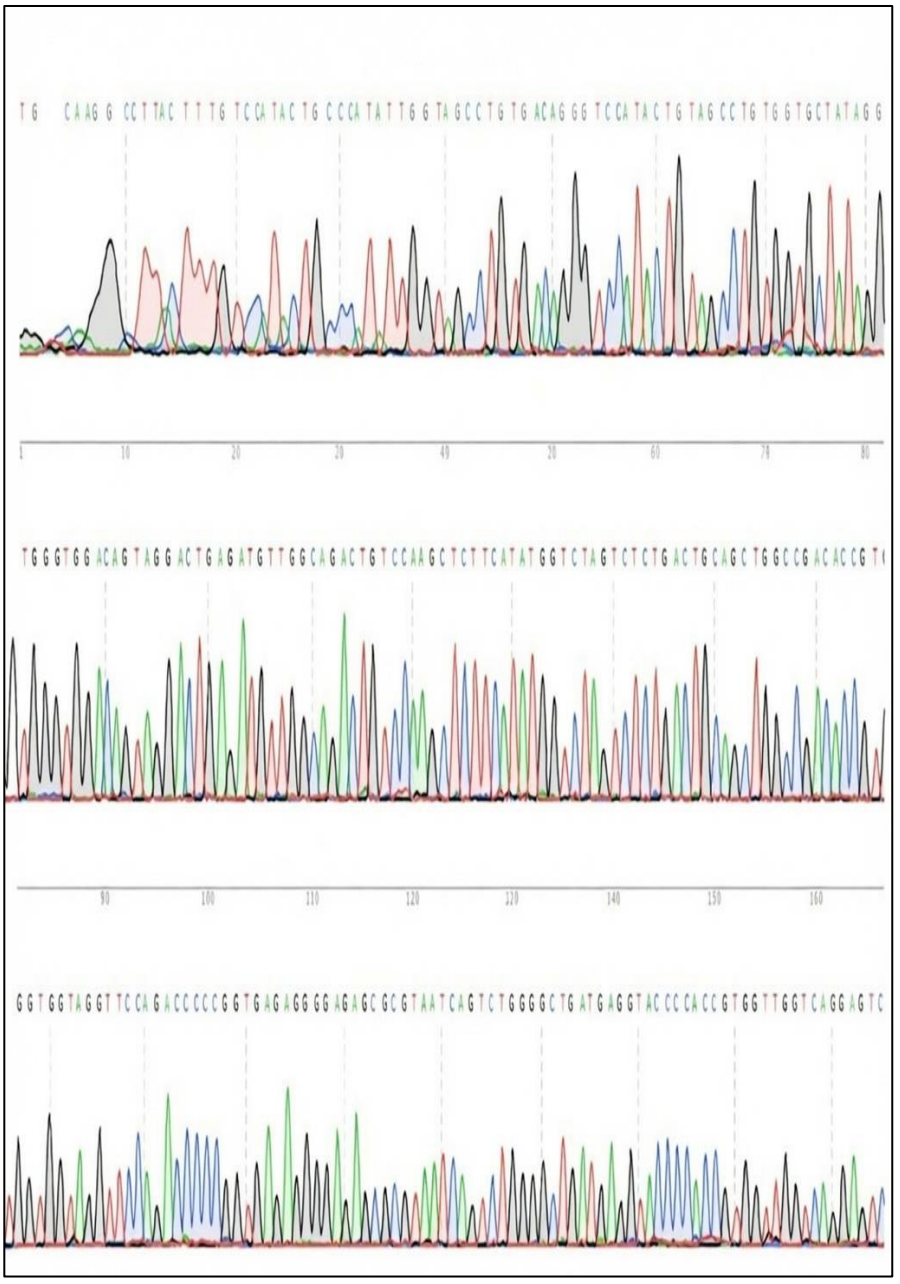

Figure: 8 Electrophoregram of exon 3 segment of the BMP4 (CasRx) gene of a participant

```
BM30 CTAGTTTGATACCTGAGACGGGGATGAAAAAAGTCGCCGAGATTCAGGGCCACGGGTG  211
BM33     CTAGTGTGATACCTGAGACGGGGAAGAAAGAAGTCGCCGAGATTCAGGGCCACGGGAG  214
BM28     CTAGTTTGATACCTGAGACGGGGAAGAAAAAAGTCGCCGAGATTCTGGGCCACGGGAG  210
BM23     CTAGTTTGATACCTGAGACGGGGAAGAAAATAGTCGCGGAGATTCAGGGCCACGGGAG  212
BM4      CTAGTTTGATACCTGAGACGGGGAAGAAAAAAGTCGCCGAGATTCAGGGCCACGGGAG  210
BM31     CTAGTTTGATACCTGAGACGGGGAAGAAAAAGGTCGCCGAGCTTCAGGGCCACGGGAG  210
BMP4     CTAGTTTGATACCTGAGATGGGGAAGAAAAAAGTCGCCGAGATTCAGGGCCACGGGAG  4799
BM1      CTAGTTTGATACCTGAGACGGGGAAGAAAAAAGTCGCCGAGATTCAGGGCCACGGGAG  208
BM2      CTAGTTTGATACCTGAGACGGGGAAGAAAAAAGTCGCCGAGATTCAGGGCCACGGGAG  209
BM20     CTAGTTTGATACCTGAGGCGGGGAAGAAAAAAGTCGCCGAGATTCAGGGCCACGGGAG  208
BM24     CTAGTTTGATACCTGAGACGGGGAAGAAAAAAGTCGCCGAGATTCAGGGCCACGGGAG  206
BM38     CTAGTTTGATACCTGAGACGGGGAAGAAAACAGTCGCCGAGATTCAGGGCCACGGGAG  209
BM27     CTAGTTTGATACCTGAGACGGGGAAGAAAAAAGTCGCCGAGATTCAGGGCCACGGGAG  208
BM3      CTCCTTTGATGCCTGTGACGGGGATGACAACGGTCGCCGAGTTTCAGTGTCGCCCGTG  207
BM25     CTTGTTTGATACCTGAGACGGGGAAGAAAAAAGTCGCCGAGATTCAGGGCCACGGGAG  209
BM26     CTGGTTTGTTACCTGAGACGGGGAAGAAAAAAGTCGTCGAGATTCAGGGCCACTGGAG  210
BM5      CTAGTCTGATACCTGAGACGGGGAAGAAAAAAGTCGCCGAGATTCAGGGCCACGGGAG  206
BM11     CTAGTTTGATACCTGAGTCGGGGAAGAAAAAAGTCGCCGAGATTCAGGGTCACGGGAG  210
```

BM11 CTAGTTTGATACCTGAGACGGGGAAGAAAAAAGTCGCCGAGATTCAGGGCCACTGGCG 210

Figure 9: Sequence alignment of amplified BMP4 gene against the NCBI database (Gene ID: 652, MIM: 112262 located on 14q22.2 with size of 7156bp).

BMP4 represents the database sequence of human. While B1-B4 represents amplified samples from study participants

Key:

Yellow: represents the codons on the human *BMP4* gene NCBI database sequence

Bright green- represents the positions of non-synonymous changes in the *BMP4* gene of the affected participant.

Aqua: represents the positions of synonymous changes in the *BMP4* gene of the affected participant**.**

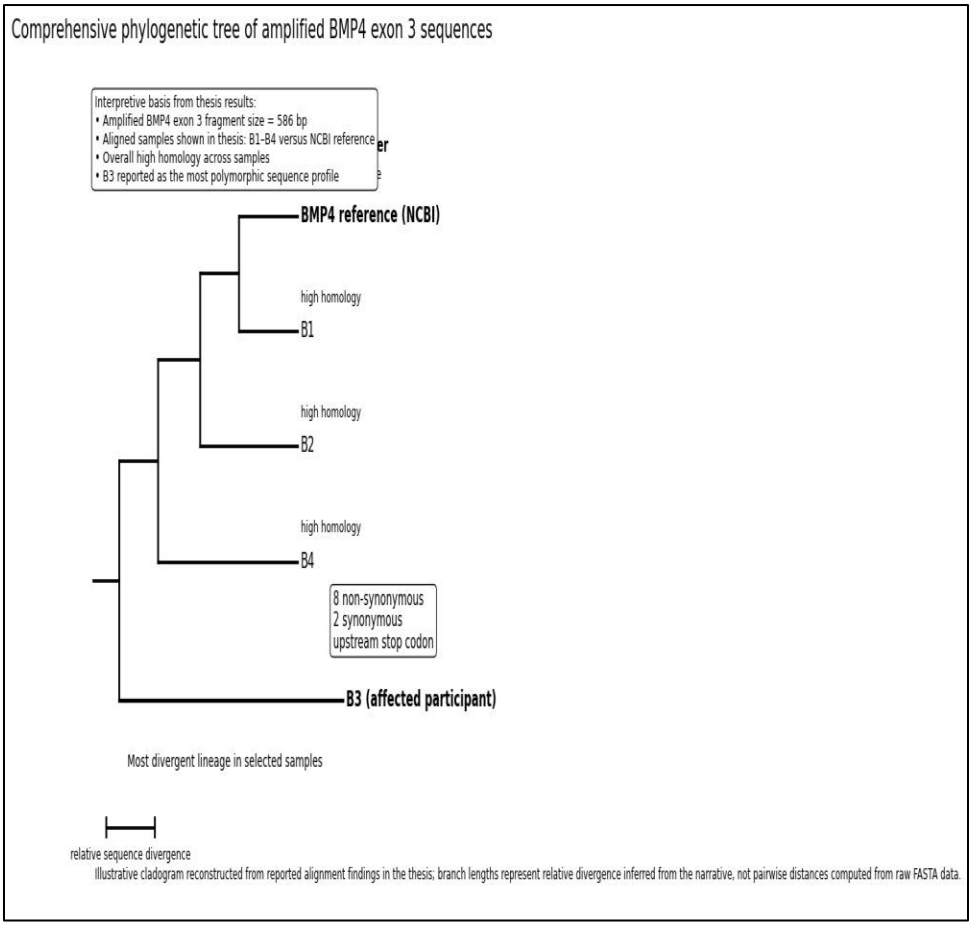

Figure 10: Phylogenetic tree of amplified BMP4 exon 3 gene sequences from selected participants (B1–B4) and the NCBI reference sequence.

Table 15: Female and Male Participants of Idomas and Igedes with Affected BMP4 Gene Values in Comparison to Overall Participant Mean Values

Measurement	Number of participants	Values for affected female participant	Mean±Standard Deviation
Nasal width (al-al)	1504	0.8464	0.5325±0.126
Morphological facial height (n-gn)	1504	1.4577	1.2040±0.353
Bizygomatic distance (zy-zy)	1504	0.8282	0.8602±0.272
Interendocanthl width (en-en)	1488	0.5354	0.5840±0.098
Ear width (l-pa)	1488	0.4706	0.6921±0.106
Ear height (sa-sba)	1484	0.8268	0.7420±0.187
Mandible height (sto-gn)	1484	0.4254	0.2940±0.240
Vermilion height (ls-sto)	1484	0.4846	0.3020±0.095
Eye fissure width* (en-ex)	1484	0.4497	0.3440±0.089

Table 16 . Female a Participants of Idomas and Igedes with Affected BMP4 Gene Values in Comparison to Overall Participant Mean Values

Measurement	Number of participants	Values for affected female participant	Mean±Standard Deviation
Nasal width (al-al)	1496	0.7062	0.8820±0.116
Morphological facial height (n-gn)	1496	1.2576	1.3060±0.272
Bizygomatic distance (zy-zy)	1496	0.9484	0.9810±0.189
Interendocanthal width (en-en)	1496	0.4455	0.6920±0.097
Ear width (t-pa)	1496	0.4717	0.6960±0.205
Ear height (sa-sba)	1496	0.9366	0.6420±0.188
Mandible height (sto-gn)	1496	0.3215	0.3940±0.240
Vermilion height (ls-sto)	1486	0.2955	0.4020±0.085
Eye fissure width* (en-ex)	1484	0.3596	0.4660±0.077
Nasal index	1484	68.8630	76.5610±0.021

Summary of Genes with Noted Variations among Idoma and Igede Participants

The molecular findings showed that selected craniofacial developmental genes exhibited identifiable sequence variations among participants. Specifically, variations were noted in the PAX3 and BMP4 genes, both of which are involved in craniofacial development and have relevance for facial, nasal, ocular, auricular, and skeletal patterning. To provide a clearer overview of these findings, the genes with noted variations, the amplified regions, types of variants, number of affected samples, and associated craniofacial observations are summarized in Table 29. As shown in Table 29, the observed genetic variations were concentrated in two craniofacial developmental genes, PAX3 and BMP4. The PAX3 findings mainly indicated synonymous changes, suggesting that the targeted region was relatively conserved across the sampled Idoma and Igede participants. In contrast, BMP4 showed both synonymous and non-synonymous changes, with participant B3 showing the most distinct sequence profile. Overall, these findings suggest that the detected gene variations are more useful for explaining individual-level craniofacial differences than for sharpsly distinguishing the two closely related ethnic populations.

Gene	Full Gene Name	Chromosomal Location / Reference Information	Targeted Region / Fragment Size	Number of Samples with Noted Variation	Type of Variation Reported	Key Participant / Sequence Observation	Craniofacial Parameters Linked with Variation	Interpretation in the Study
PAX3	Paired Box Protein 3	Chromosome 2q35	Exon 8 region; expected PCR fragment size of 311 bp	34 / 300	Mostly synonymous mutations; one participant was noted to have non-synonymous changes	Participant P15 was reported as having notable non-synonymous variations in the targeted *PAX3* region	Nasal width, canthal-related dimensions, and other facial, nasal, auricular, and craniofacial measurements	*PAX3* variations did not clearly separate Idoma from Igede participants but may explain individual-level craniofacial deviations within the shared population background
BMP4	Bone Morphogenetic Protein 4	NCBI Gene ID: 652; MIM: 112262; located on 14q22.2; gene size reported as 7156 bp	Exon 3 region; expected PCR fragment size of 586 bp	22 / 300	Both synonymous and non-synonymous variations; stop codon also reported upstream of the target sequence	Participant B3 showed the most distinct sequence variation and formed the most divergent branch on phylogenetic analysis; B1, B2, and B4 clustered closer to the NCBI *BMP4* reference	Morphological facial height, bizygomatic distance, interendocanthal width, ear width, ear height, mandible height, eye fissure width, and nasal index	*BMP4* variation may be associated with observable craniofacial differences, especially individual deviations from the overall population mean, but it did not form a sharp ethnic boundary between Idoma and Igede participants

Discussion

Each face characteristic, such as the size, shape, and spatial orientation of the eyes, nose, mouth, ears, and other features, distinguishes one individual from another (Richmond et al., 2018), and these facial features are among the most recognizable human traits with considerable hereditary influence (Pandya et al., 2024). Thus, the findings of this study on craniofacial

anthropometric indices, together with the single nucleotide polymorphism loci identified in the PAX3 and BMP4 genes as genetic markers, provide useful identification tools for describing the Idoma and Igede populations of Benue State, Nigeria.

In this present study, a total of 3,000 participants took part in the anthropometric assessment. The demographic distribution showed an almost equal representation of the sexes, with 1,504 males (50.1%) and 1,496 females (49.9%), giving a male-to-female ratio of approximately 1:1. The ethnic distribution showed that 1,800 participants (60.0%) were Idoma and 1,200 (40.0%) were Igede. The near-equal sex distribution was useful for the assessment of sexual dimorphism, while the inclusion of substantial numbers from both ethnic groups provided an adequate basis for comparing their craniofacial patterns.

In addition, when the participants were grouped into age categories, adolescents aged 15-19 years accounted for 986 (32.9%), young adults aged 20-24 years accounted for 1,016 (33.9%), and adults aged 25-29 years accounted for 998 (33.3%), with a mean age of 22.0 ± 4.1 years. The choice of these age groups is appropriate for craniofacial assessment because most major facial growth is completed by late adolescence and early adulthood, while the more pronounced changes associated with ageing and soft-tissue laxity occur later in life (Al-Taai et al., 2022). Also, at this period the main growth at the cranial base is largely completed and age-related facial sagging is minimal.

In this study, covariate factors such as weight, height, and body mass index (BMI), which could produce false-positive interpretations, were also taken into consideration (Table 23). The participants had a mean height of 1.67 m and a mean weight of 62.6 ± 11.8 kg. The overall mean BMI was 23.6033 ± 1.77743 kg/m², and the largest group, 2,116 participants, was within the normal BMI category with a mean BMI of 21.4367 ± 1.58042 kg/m². Only 8 participants were underweight, 591 were overweight, and 285 were obese. The result therefore showed that most participants were of normal weight and that BMI was unlikely to have had a major effect on the craniofacial parameters studied.

The correlation analysis further showed that BMI had only weak relationships with the craniofacial indices. Facial index (FI) had a weak positive correlation with BMI (r = 0.09), nasal index (NI) also had a weak positive correlation (r = 0.11), canthal index (CI) had a weak negative correlation (r = -0.06), and ear index (EI) had a very weak positive correlation (r = 0.04). The present findings differ from reports in which facial traits showed moderate relationships with BMI and body composition, but the difference may be explained by the fact that BMI, height, and fat distribution vary according to sex, age, genetic background, and the type of facial measurement used (Jeong et al., 2023).

Our results on facial index showed that the hyperleptoprosopic (very long face) was the commonest facial category in both populations and in both sexes. Among the Idoma, 26.2% of males and 27.0% of females were hyperleptoprosopic, while among the Igede, 26.9% of males and 24.8% of females fell into this category. Few differences were observed in the remaining face types, and broader face categories were only slightly more frequent in some male groups. The pattern is consistent with the concept that population groups may share a dominant facial form while differing in the relative frequencies of the less common facial categories (Richmond et al., 2018).

Also, when the mean FI values of the present study were compared, Idoma males had a mean facial index of 88.45 ± 4.72 and Igede males had 87.81 ± 4.55, whereas Idoma females had 85.67 ± 4.28 and Igede females had 86.12 ± 4.41. The male values were generally higher than the female values, especially among the Idoma, indicating sexual dimorphism in facial proportion. The slight differences between the Idoma and Igede means also show an ethnic influence, although the degree of overlap suggests that the two populations are more similar than different in their general facial form.

The FI values indicated that the two populations were distributed mainly around long and very long facial categories. When these findings are considered alongside reports from other populations, they support the view that facial type varies across sex, ancestry, geography, and measurement method. Some populations have been reported to show a predominance of mesoprosopic or euryprosopic faces, while others show leptoprosopic or hyperleptoprosopic patterns. The differences across studies may be due to ethnic and racial variation, the age range studied, and whether the measurements were obtained with calipers, two-dimensional photographs, three-dimensional images, or skeletal landmarks (Nguyen et al., 2024).

The age analysis of FI showed mean values of 86.45 ± 4.80 for participants aged 15-19 years, 87.12 ± 4.90 for those aged 20-24 years, and 88.05 ± 5.00 for those aged 25-29 years. This showed a mild increase with age, but the hyperleptoprosopic category remained predominant across the age groups. The correlation of age with FI was weak (r = 0.12), which suggests that the facial index was relatively stable from adolescence to the end of the third decade in the present population. This agrees with the view that the major pattern of facial morphology is established by late adolescence, although small proportional changes may continue into adulthood (Sharma et al., 2014).

The findings of this study on FI can be applied in forensic medicine, plastic and maxillofacial surgery, diagnostic comparison between patients and healthy individuals, facial reconstruction, and personal identification, particularly where sex- and population-specific reference values are required. However, because the Idoma and Igede values overlapped substantially, FI should be combined with other craniofacial measurements and genetic information rather than used as a single ethnic discriminator.

Nasal index showed that the hyperplatyrrhine (very broad broad) nose was the most frequent nasal type among both Idoma and Igede males and females. Idoma males recorded 38.7% hyperplatyrrhine, 34.9% mesorrhine, 13.9% platyrrhine (broad), and 12.7% leptorrhine nasal types. Idoma females recorded 41.1% hyperplatyrrhine, 31.6% mesorrhine, 17.2% platyrrhine, and

10.1% leptorrhine. Among the Igede, males recorded 39.9% hyperplatyrrhine and females 41.3%, while the leptorrhine type remained the least frequent. The findings therefore showed a common broad nasal pattern in the two populations.

Furthermore, differences in the mean NI values showed that Idoma males had 92.34 ± 6.85 and Igede males had 94.12 ± 6.71, while Idoma females had 93.89 ± 6.52 and Igede females had 95.67 ± 6.78. The Igede values were slightly higher than the corresponding Idoma values, and the female values were also slightly higher than the male values within each group. These results demonstrate both sexual and ethnic variation, although the differences were modest and all four groups remained within broad nasal categories.

According to age groups, the mean nasal index increased from 93.67 ± 6.75 among participants aged 15-19 years to 94.23 ± 6.82 among those aged 20-24 years and 95.14 ± 6.95 among those aged 25-29 years. Hyperplatyrrhine nasal form remained the dominant category across the age groups and in both ethnic populations. Thus, even though a small increase in the mean NI was observed with age, the general nasal form did not change substantially within the age range studied.

Anthropological studies have shown that the form of the nose is influenced by both ancestry and climate. Broader nasal forms are frequently reported in warm and humid environments, while narrower forms are more common in cold and dry climates because of differences in the conditioning of inspired air (Zaidi et al., 2017). The predominance of hyperplatyrrhine and platyrrhine forms among the Idoma and Igede is therefore compatible with their shared tropical environment in Benue State. The similarity between the two populations also suggests that geographical proximity and shared ecological exposure may contribute to the observed pattern.

Considering the covariates, NI showed a weak positive correlation with BMI (r = 0.11), a weak negative correlation with age (r = -0.08), and a positive relationship with gender (r = 0.18). These results suggest that sex contributes more to nasal variation than age or BMI in the present population. The findings also support the observation that nasal morphology is influenced by genetic background and sexual dimorphism rather than by body size alone (Premraj et al., 2025).

The normative data on NI obtained in this study are valuable in rhinoplastic surgery, the assessment of craniofacial anomalies such as cleft lip and palate that are associated with nasal deformity, biological profiling, facial reconstruction, and ethnic and population identification. Nevertheless, because the nasal categories of the Idoma and Igede overlap, nasal index should be interpreted as part of a combined identification profile.

Canthal index analysis showed that the close-eye pattern was the dominant category in the categorical tables for both populations and both sexes, while far-apart eyes were absent or extremely rare. Among Idoma females, 66.7% had close eyes, 33.2% had intermediate spacing, and 0.1% had far-apart eyes. Among Idoma males, 69.2% had close eyes and 30.8% had intermediate spacing. Igede females recorded 71.2% close eyes and 28.8% intermediate eyes, while Igede males recorded 64.5% close eyes and 35.5% intermediate eyes. No far-apart eyes were recorded among the Igede participants.

The mean CI values were 37.82 ± 2.65 for Idoma males, 37.45 ± 2.48 for Igede males, 38.56 ± 2.71 for Idoma females, and 38.21 ± 2.59 for Igede females. The female means were slightly higher than the male means, but the differences were small. Although the group means fell close to the intermediate category, the categorical crosstab showed a predominance of close-eye spacing. This apparent difference reflects the effect of classification cut-off points and the distribution of individual observations around the group mean.

When CI was considered according to age group, close-eye spacing remained the most common pattern. Among the Idoma, close eyes accounted for 89.3% in the 15-19 year group, 90.9% in the 20-24 year group, and 91.9% in the 25-29 year group. Among the Igede, the corresponding proportions were 87.3%, 89.5%, and 90.2%. The mean CI also changed only slightly from 37.89 ± 2.68 to 37.95 ± 2.71 and 38.12 ± 2.74 across the three age groups.

The present findings therefore show that close and intermediate eye spacing are the dominant canthal patterns in the Idoma and Igede populations. The small differences between the male and female means suggest modest sexual dimorphism, while the high degree of overlap between the ethnic groups indicates that CI alone cannot reliably distinguish an Idoma individual from an Igede individual. This is in keeping with the observation that regional and genetic factors can produce both shared and population-specific ocular proportions (Han et al., 2024).

The age correlation of CI was weak (r = 0.05), and BMI showed a weak negative correlation (r = -0.06). Gender had a slightly stronger but still modest relationship (r = 0.15). These findings indicate that canthal proportion was relatively stable in the age range studied and was not meaningfully influenced by BMI. The stability of the canthal relationship during young adulthood makes it useful for normative comparison, even though its discriminatory value between these two closely related populations is limited.

The anthropometric data on CI are valuable in the assessment of craniofacial syndromes, the treatment of post-traumatic canthal deformity, the evaluation of hypertelorism and telecanthus, the design of spectacles and ocular devices, and the clinical recognition of conditions in which canthal displacement is a feature. In forensic work, the measurement may contribute to facial reconstruction and biological profiling when interpreted together with nasal, facial, auricular, and genetic findings (Adekunle et al., 2022).

The ear index was also determined in this study. The results revealed that large, narrow, and long ears were the most common ear type in both populations and both sexes, while small ears were the least frequent. Large ears were observed in 75.5% of

Idoma females, 76.2% of Idoma males, 74.2% of Igede females, and 75.7% of Igede males. Medium ears accounted for approximately 17-18% of each group, whereas small ears accounted for only about 6-8%.

The mean EI for Idoma males was 57.23 ± 3.94 and that of Igede males was 56.89 ± 3.81, while Idoma females had 56.45 ± 3.82 and Igede females had 55.98 ± 3.69. The male values were slightly higher than the female values in both populations. These results demonstrate modest sexual dimorphism but also show considerable overlap between the Idoma and Igede. The findings are consistent with the general observation that auricular dimensions vary by sex and ancestry, while neighbouring populations may share closely similar proportions(Mahawar et al., 2026).

When age was taken into consideration, large ears remained predominant across all groups. Among the Idoma, large ears were recorded in 90.3% of participants aged 15-19 years, 89.9% of those aged 20-24 years, and 88.9% of those aged 25-29 years. Among the Igede, the corresponding proportions were 88.3%, 89.9%, and 90.1%. The mean EI values were 56.78 ± 3.92, 56.45 ± 3.85, and 56.12 ± 3.88 across the age groups. The small differences did not alter the dominant auricular classification.

The findings should be considered in relation to reports that the exteRNAl ear continues to change throughout life through cartilage growth and tissue remodelling (Anthwal & Thompson, 2016). The present age range ended before 30 years and therefore did not include older adults in whom age-related auricular changes may be more pronounced. Within the present population, age had only a weak correlation with EI (r = 0.09), while BMI had a very weak correlation (r = 0.04).

The knowledge of the normative data on EI is useful in the diagnosis of craniofacial syndromes, auricular reconstruction, the provision of support for spectacles, the design of hearing aids, earbuds, and other ear-worn devices, and forensic identification. Population-specific data are particularly important because ear size and proportion differ among sex, age, and ancestry groups (Rani et al., 2020).

When the findings of this study were compared across the indices, sexual dimorphism was present, but the differences between the Idoma and Igede were generally small. Gender showed weak but statistically meaningful correlations with FI (r = 0.21), NI (r = 0.18), and EI (r = 0.17), whereas age and BMI showed weaker and mostly non-significant relationships. The dominant categories in both populations were hyperleptoprosopic face, hyperplatyrrhine nose, close or intermediate eye spacing, and large ears. These results indicate that the strongest differences were sex-related and individual rather than sharply ethnic.

Craniofacial abnormalities and normal facial variation have underlying genetic and environmental components (dbGaP Study, n.d.; M. K. Lee, Warburton, et al., 2017). The genetic basis of craniofacial embryogenesis is complex, but associations have been demonstrated between developmental genes and measurements such as facial width, nasal form, canthal spacing, mandibular dimensions, and auricular proportions. The present study therefore focused on genetic changes in PAX3 and BMP4, two genes known to participate in normal craniofacial development.

In the two genes evaluated, variations were associated with differences in twelve linear measurements and one index. The affected participants differed from the overall population means in nasal width, nasal height, morphological facial height, bizygomatic distance, interendocanthal width, ear width, ear height, mandible height, mouth width, vermillion height, eye fissure width, and nasal index. The results are in line with studies showing that variants in craniofacial developmental genes may be associated with facial breadth, nasal dimensions, ocular spacing, and mandibular morphology (Kareem et al., 2025b).

Amplification of the targeted PAX3 region produced the expected 311 bp fragment. Sequence alignment showed high similarity across the study population, and 34 of the 300 samples showed noted variation, most of which was synonymous. The sequence profile of the most affected participant showed substantially more polymorphism than the other samples and was reported to contain 22 non-synonymous variations within the targeted region. The coding-region translation analysis also identified five non-synonymous substitutions, Y453N, S454I, D461Y, V463D, and Y466S, together with two synonymous variants and a localized haplotype transition from YSTTG to EHHGH.

These changes were concentrated within the selected PAX3 region and therefore should be interpreted in relation to the region amplified and sequenced. PAX3 is a large gene, and mutation positions differ from one study to another according to the exon, intron, or regulatory segment under investigation. The present findings nevertheless demonstrate that single-base substitutions, insertions, deletions, and haplotype changes can occur within the PAX3 sequence of the study population.

Point mutations and other sequence variations in PAX3 were accompanied by differences in craniofacial measurements. The affected participants showed changes in nasal width and height, facial height, bizygomatic distance, interendocanthal width, ear dimensions, mandibular height, mouth width, vermillion height, eye fissure width, and nasal index when compared with the overall means. These differences may influence the phenotypic appearance of the affected individuals, even where a classical craniofacial syndrome is not clinically obvious.

The absence of an obvious classical appearance among the affected participants may be related to the extent of the sequence change, the location of the variant, gene dosage, modifier genes, or environmental and epigenetic influences. PAX3 mutations are known to have variable expression, and the same developmental pathway may produce a broad spectrum ranging from subtle facial variation to a recognizable syndrome. Therefore, the presence of a sequence variant does not by itself establish a clinical diagnosis.

The findings of this study cannot categorically state that any affected participant had Waardenburg syndrome or another PAX3-related disorder. The purpose of the study was to determine whether PAX3 could serve as a useful marker for predicting or

explaining facial appearance among the Idoma and Igede populations, rather than to diagnose a syndrome. The findings support the use of objective craniofacial measurements for describing subtle genotype-phenotype relationships rather than depending on visual judgement alone.

PAX3-related disorders may include dystopia canthorum, broad nasal root, altered nasal tip, mandibular changes, pigmentation abnormalities, and other craniofacial features. In the present study, the affected participants had values that differed from the population means in facial, nasal, ocular, mandibular, and auricular dimensions. These deviations could represent subtle expressions of altered PAX3 function, but clinical examination and family studies would be required before any diagnostic conclusion could be made (Boudjadi et al., 2018b).

Among the affected Idoma male participants, the following indices measured in centimeter(cm), nasal width was 38.6 compared with an overall male mean of 35.2, nasal height was 50.2 compared with 46.8, morphological facial height was 118.4 compared with 112.6, bizygomatic distance was 132.7 compared with 126.5, and nasal index was 91.6 compared with 86.9. The affected Idoma females also showed higher values, including a facial height of 115.2 compared with 110.4 and a bizygomatic distance of 128.6 compared with 122.9. These differences support an association between PAX3 variation and measurable craniofacial deviation.

The Igede participants with the following indices measured in centimeters (cm) showed the same general direction of change. Affected Igede males had nasal width of 39.8 compared with 36.1, nasal height of 51.6 compared with 47.5, facial height of 120.5 compared with 114.2, bizygomatic distance of 134.9 compared with 128.3, and nasal index of 93.1 compared with 87.4. Affected Igede females had facial height of 116.7 compared with 111.1 and bizygomatic distance of 129.8 compared with 124.0. The consistency of these deviations in both populations suggests an individual genotype-phenotype effect rather than an ethnic-specific effect.

The interendocanthal width of affected PAX3 participants was also higher than the corresponding population means. The affected Idoma male value was 32.5 compared with 30.1, the Idoma female value was 31.7 compared with 29.8, the Igede male value was 33.2 compared with 30.8, and the Igede female value was 32.1 compared with 30.0. This finding is relevant because PAX3 has an established role in neural crest development and the formation of the nasal root and orbital region (Prince et al., 2026).

The phylogenetic analysis of PAX3 showed tight clustering and shallow branching in most samples, which confirms the high level of sequence similarity across the Idoma and Igede populations. Small sequence clusters were associated with multiple substitutions, and shared insertion or deletion patterns were present in some samples. A few sequences, including Px42, Px45, and Px46, contained larger regions of missing bases. These clusters may indicate individual or sub-population variation, but they did not form a clear genetic boundary between the two ethnic groups.

The study also identified polymorphisms in the BMP4 gene that were associated with craniofacial measurements differing from the overall population means. Amplification of exon 3 produced the expected 586 bp fragment, and sequence alignment showed a high level of homology across the population. 22 of the 300 samples exhibited synonymous and non-synonymous variation. Participant B3 had the most distinct sequence profile and formed the most divergent branch on phylogenetic analysis, while B1, B2, and B4 clustered more closely with the NCBI reference sequence.

The affected BMP4 participant was reported to have eight non-synonymous and two synonymous changes within exon 3, together with a stop codon upstream of the target sequence. A premature stop signal or a non-synonymous substitution may alter the amino-acid sequence, protein folding, or the quantity of functional BMP4 protein(Kristofich et al., 2018). This is biologically plausible because BMP4 is a major regulator of neural crest development, maxillary and mandibular growth, epithelial-mesenchymal interaction, and craniofacial skeletal patterning (Kristofich et al., 2018).

The study also reported two recurring BMP4 SNP patterns in the sequence subset: an AGT-to-AAT change at nucleotide position 481, associated with an S25N codon change and observed in 165 of 300 samples (55.0%), and a CGG-to-AGG change at position 571, reported in 170 of 300 samples (57%). In total, 186 of 300 samples (62%) carried one or more of the listed SNPs in that analysis. These frequencies describe variants within the tested sequence subset and should not be interpreted as the prevalence of a congenital disorder.

The synonymous changes found within the BMP4 region may not alter the encoded amino acid, but they may still influence messenger RNA stability, translation efficiency, splicing, or protein expression in some circumstances(Kristofich et al., 2018; Oelschlaeger, 2024). The non-synonymous changes and the upstream stop codon are more likely to have functional effects, although functional laboratory studies would be required to establish their biological consequences. The present findings therefore show association and sequence diversity, but they do not by themselves prove causation.

In the present study, affected BMP4 participants displayed craniofacial values above the corresponding overall means. Affected females had morphological facial height of 116.7 compared with 111.1 ± 5.4, bizygomatic distance of 129.8 compared with 124.0 ± 4.8, interendocanthal width of 32.1 compared with 30.0 ± 2.1, ear height of 62.0 compared with 58.3 ± 3.1, and nasal index of 91.2 compared with 86.2 ± 4.3. These results suggest that BMP4 variation may be associated with differences in facial, orbital, auricular, and mandibular dimensions.

Affected males showed a similar pattern, with morphological facial height of 119.8 compared with 114.2 ± 5.9, bizygomatic

distance of 133.6 compared with 128.3 ± 5.2, interendocanthal width of 33.0 compared with 30.8 ± 2.3, ear height of 63.5 compared with 60.1 ± 3.4, mandible height of 71.2 compared with 67.9 ± 4.0, and nasal index of 92.8 compared with 87.4 ± 4.6. The parallel direction of change in males and females supports an individual-level relationship between BMP4 variation and craniofacial morphology.

The incidence of detected PAX3 and BMP4 sequence variation in this study should be distinguished from the prevalence of clinical disorders associated with these genes. 34 of 300 PAX3 samples and 22 of 300 BMP4 samples showed noted variation, but only selected participants displayed a highly polymorphic pattern and measurable craniofacial deviation. Most variants were synonymous or occurred in individuals without a classical syndrome. Therefore, the findings should be interpreted as population genetic variation and possible genotype-phenotype association rather than as evidence that the participants had Waardenburg syndrome, anophthalmia, microphthalmia, or another congenital condition(Aboagye et al., 2025).

Thus, the findings highlight the fact that DNA sequences of PAX3 and BMP4 are potential genetic markers for craniofacial morphology in the Idoma and Igede populations. Their greatest value in the present data lies in explaining individual differences and supporting a combined biological profile. Neither gene produced a sharp ethnic separation between the two groups, which is consistent with the extensive overlap observed in the craniofacial indices.

Future studies should use genome-wide association studies, larger molecular samples, and additional craniofacial developmental genes to understand the diversity of these markers and their influence on facial morphology. Longitudinal and family-based studies would also help determine inheritance patterns and the clinical significance of the variants. Individuals with marked PAX3 or BMP4 variation may benefit from appropriate clinical review and genetic counselling where a relevant phenotype or family history is present.

The predictive potential of genetic markers that influence facial morphology is important for estimating the appearance of an unknown individual from DNA recovered at a crime scene or from unidentified remains. However, the results of this study show that prediction should be based on a panel of markers and several anthropometric traits rather than on PAX3, BMP4, or a single facial index alone. The combination of craniofacial measurements, sex, age, ancestry information, and molecular data will provide a more reliable forensic interpretation (New et al., 2025).

This study concluded that normative craniofacial indices, dysmorphological craniofacial measurements, and DNA sequences of PAX3 and BMP4 are useful tools for identifying and biologically describing people in Nigeria. The sequences of PAX3 and BMP4 were highly similar across the Idoma and Igede populations, with minor changes that were mainly synonymous in most participants. The distinctive non-synonymous changes were associated principally with individual deviations from the population means. The anthropometric and molecular findings therefore provide useful population-specific data, but accurate differential identification of Idoma and Igede individuals will require the combined use of several craniofacial and genetic markers.

Conclusions

The study found that very long facial forms, broad nasal types, close to intermediate eye spacing, and large ear sizes are the predominant craniofacial features among the Idoma and Igede populations. The similarities in craniofacial indices indicate a shared regional profile, with only minor differences due to sex and individual variation. Genetic variations in the PAX3 and BMP4 genes were associated with differences in craniofacial traits, supporting their role in individual identification. However, these genetic markers alone were insufficient to clearly distinguish between the two ethnic groups. Therefore, accurate forensic identification should integrate multiple craniofacial measurements, demographic factors, and a combination of genetic markers rather than relying on a single parameter.

References

1. Adhikari, K., Fuentes-Guajardo, M., Quinto-Sánchez, M., Mendoza-Revilla, J., Chacón-Duque, J. C., Acuña-Alonzo, V., Jaramillo, C., Arias, W., Lozano, R. B., Pérez, G. M., Gómez-Valdés, J., Villamil-Ramírez, H., Hunemeier, T., Ramallo, V., Silva de Cerqueira, C. C., Hurtado, M., Villegas, V., Granja, V., Gallo, C., … Ruiz-Linares, A. (2016). A genome-wide association scan implicates DCHS2, RUNX2, GLI3, PAX1, and EDAR in human facial variation. Nature Communications, 7, Article 11616. https://doi.org/10.1038/ncomms11616
2. Claes, P., Liberton, D. K., Daniels, K., Rosana, K. M., Quillen, E. E., Pearson, L. N., McEvoy, B., Bauchet, M., Zaidi, A. A., Yao, W., Tang, H., & Shriver, M. D. (2014). Modeling 3D facial shape from DNA. PLoS Genetics, 10(3), e1004224. https://doi.org/10.1371/journal.pgen.1004224
3. Qian, Y., et al. (2022). Genome-wide association studies of human facial morphology. Nature Communications, 13, Article 1–12.
4. Richmond, S., Zhurov, A. I., & others. (2018). 3D facial analysis and population variation. Orthodontics & Craniofacial Research, 21(Suppl. 1), 1–8.
5. Barash, M., et al. (2016). Forensic DNA phenotyping: Current state of the art. Forensic Science International: Genetics, 23, 1–12.

6. Barash, M., et al. (2018). Forensic DNA phenotyping: Current applications and future directions. Trends in Biotechnology, 36(6), 1–10.
7. de Boer, J., et al. (2019). Advances in forensic DNA phenotyping. Forensic Science International: Genetics, 39, 1–10.
8. Pollard, K. S., et al. (2022). Genetic determinants of human facial traits. Nature Genetics, 54, 1–10.
9. Adekunle, A. A., Olowo, A. Y., James, O., Adamson, O. O., Alade, A. A., Agbogidi, F. O., Oladega, A. O., Ogunlewe, M. O., Adeyemo, W. L., Busch, T. D., Mossey, P. A., Marazita, M. L., & Butali, A. (2022). Facial anthropometry measurements using 3D stereophotogrammetry analysis among Nigerians. Journal of Craniofacial Surgery, 33(4), 1178–1181. https://doi.org/10.1097/SCS.0000000000008036
10. Bhupathi, V., & Ravi, K. (2017). Anthropometric study of craniofacial features. Journal of Clinical and Diagnostic Research, 11(5), 1–5.
11. David, O., et al. (2020). Craniofacial indices and anthropometric variations. Anatomy Research International, 1–8.
12. Mehta, P. (1997). Anthropometric study of facial parameters. Journal of Anatomy, 191, 1–10.
13. Matthews, R., et al. (2024). Recent advances in craniofacial genetics. Human Biology, 96(2), 1–12.
14. Abdulrazzaq, Y. M., Aburawi, E., Abdulrahman, M., Alshamsi, A., & Zidan, M. (2026). A comparative analysis of BMI and skinfold measurements in the assessment of body composition parameters. Scientific Reports, 16, 6191. https://doi.org/10.1038/s41598-026-37549-0
15. Aboagye, E. T., Wonkam, R. P., Kock, C. de, Dandara, C., & Wonkam, A. (2025). Genetics of Waardenburg syndrome in Africa: A systematic review. International Journal of Molecular Sciences, 27(1). https://doi.org/10.3390/ijms27010127
16. Abushehab, A., Rames, J. D., Hussein, S. M., Meira Pazelli, A., Sears, T. A., Wentworth, A. J., Morris, J. M., & Sharaf, B. A. (2024). Midface skeletal sexual dimorphism: Lessons from 3D imaging. Plastic and Reconstructive Surgery Global Open, 12(10), 6215. https://doi.org/10.1097/GOX.0000000000006215
17. Acharya, S., Gupta, C., Palimar, V., Kalthur, S. G., & Adhikari, P. (2025). Morphological and morphometric analysis of the human external ear. F1000Research, 14, 119. https://doi.org/10.12688/f1000research.160629.3
18. Agbolade, O., Nazri, A., Yaakob, R., Ghani, A. A., & Cheah, Y. K. (2019). 3D facial expression recognition using multipoints warping. BMC Bioinformatics, 20, 619. https://doi.org/10.1186/s12859-019-3153-2
19. Al-Bitar, Z. B., Hamdan, A. M., Shqaidef, A., Garagiola, U., & Naini, F. B. (2023). Perception of frontal facial images vs mirror images. Maxillofacial Plastic and Reconstructive Surgery, 45(1), 29. https://doi.org/10.1186/s40902-023-00396-4